# Appendix-Integrated CT/MRI Diagnostic System for Pancreatic Cystic Lesions Supporting Pathological Classification and Risk Stratification

Xiaonan Cui, Houpu Liu, Sunyi Zheng, Hongwei Wang, Jiaxin Liu, Ziyi Gao, Tianye Liu, Jing Liang, Xinru Zheng, Jing Wang, Keyi Bian, Xiaomeng Yang, Chunlin Zhang, Tianshuo Jiao, Yufei Yang, Shuxuan Fan, Xiuchao Wang, Song Gao, Chuntao Gao, Yukuan Feng, Hui Li, Guoping Xu, Xiang Zhang, Wen Shen, Haoran Sun, Baocun Sun, Yan Sun, Jianyu Xiao, Yalin Zheng, Michael Ying, Geertruida H de Bock, Zhaoxiang Ye, Jihui Hao

Appendix 1. Main variable definitions and schematic depicting representative main imaging features of PCL....3

1.1 Pathological classification & risk stratification criteria....3

1.2 Schematic depicting representative main imaging features of PCLs....5

Appendix 2. Data processing, feature selection, and study size....15

2.1 Data processing and inter-rater reliability assessment....15

2.2 Handling of missing data: multiple imputation....18

2.3 Feature selection....20

2.4 Sample size....23

2.5 Decision curve analysis....25

Appendix 3. Demographic tables for the three models....26

Appendix 4. Pathological classification model development and temporal validation....43

4.1 Model overview....43

4.2 Standardization parameters....43

4.3 Prediction score formulas for pathological classification prediction....45

4.4 SHAP analysis and DCA analysis for the five category model....49

Appendix 5. IPMN risk stratification model development and temporal validation. 54

5.1 Model overview....54

5.2 Standardization parameters....54

5.3 Prediction score formulas for IPMN risk prediction....56

5.4 SHAP analysis and ROC curve for the IPMN risk stratification model ..... 58

Appendix 6. MCN risk stratification model development and temporal validation .. 63

6.1 Model overview ..... 63

6.2 Standardization parameters ..... 63

6.3 Prediction score formulas for MCN risk prediction ..... 64

6.4 SHAP analysis and ROC curve for the MCN risk stratification model 66

Appendix 7. Subgroup analysis conducted in full datasets without MICE ..... 71

Appendix 8. Clinical application of SIRS-PCLs: case demonstrations of pathological five-category classification and risk stratification ..... 74

## Appendix 1. Main variable definitions and schematic depicting representative main imaging features of PCL

*1.1 Pathological classification & risk stratification criteria*

The risk classification for IPMN and MCN is assigned according to histopathological findings in accordance with the 2019 World Gastroenterology Organization (WGO) practice guideline for PCLs (Table S1).

Table S1. Pathological classification & risk stratification criteria.

| Class | Group | Subgroups | Type | Risk stratification model[1] |
|---|---|---|---|---|
| **Serous cystic neoplasm (SCN)** | 1 Serous cystadenoma | a Serous microcystic adenoma | Benign | Benign |
| | | b Serous oligocystic adenoma | | |
| | 2 Serous cystadenocarcinoma | | Malignant | High Risk |
| **Mucinous cystic neoplasm (MCN)** | 1 Mucinous cystadenoma | | Benign | Benign |
| | 2 Mucinous cystic neoplasm | a Low-grade | Borderline | Low Risk |
| | | b High-grade* | Carcinoma in situ | Medium Risk |
| | 3 Mucinous cystadenocarcinoma | a Noninvasive | Malignant | High Risk |
| | | b Invasive | | |
| **Intraductal papillary mucinous neoplasm (IPMN)** | 1 Intraductal papillary mucinous neoplasm | a Low-grade | Borderline | Low Risk |
| | | b High-grade* | Carcinoma in situ | Medium Risk |
| | 2 Intraductal papillary mucinous carcinoma | a Noninvasive | Malignant | High Risk |
| **Solid pseudopapillary neoplasm (SPN)[2]** | 1 Solid pseudopapillary neoplasm | | Borderline | Medium Risk |
| | 2 Solid pseudopapillary carcinoma | | Malignant | High Risk |
| **Neuroendocrine tumors (NET)[2]** | 1 Neuroendocrine tumors | G1, G2 | | Medium Risk |
| | | G3 | | High Risk |
| | 2 Neuroendocrine carcinoma | | | |

[1] The risk stratification principles of our model are derived from an expert consensus formula based on the 2019 WHO Classification of Tumours of the Digestive System and the 2019 WGO Practice Guideline for Pancreatic Cystic Lesions. Accordingly, lesions are categorized as follows:

- Benign: Lesions can be managed with annual follow-up.
- Low risk: Lesions with low-grade malignant potential, requiring close surveillance.
- Medium risk: Lesions requiring further diagnostic evaluation (e.g., endoscopic ultrasound - ESG) for clarification.
- High risk: Lesions suspected to be malignant, for which surgical intervention is recommended

[2] Given the clear clinical indication for surgical intervention in both solid pseudopapillary neoplasms (SPN) and neuroendocrine tumors (NET), our risk stratification model does not include a "low-risk" category for these entities. Following multidisciplinary team (MDT) consultation, surgical resection is recommended for all cases where SPN or NET is strongly suspected.

*1.2 Schematic depicting representative main imaging features of PCLs*

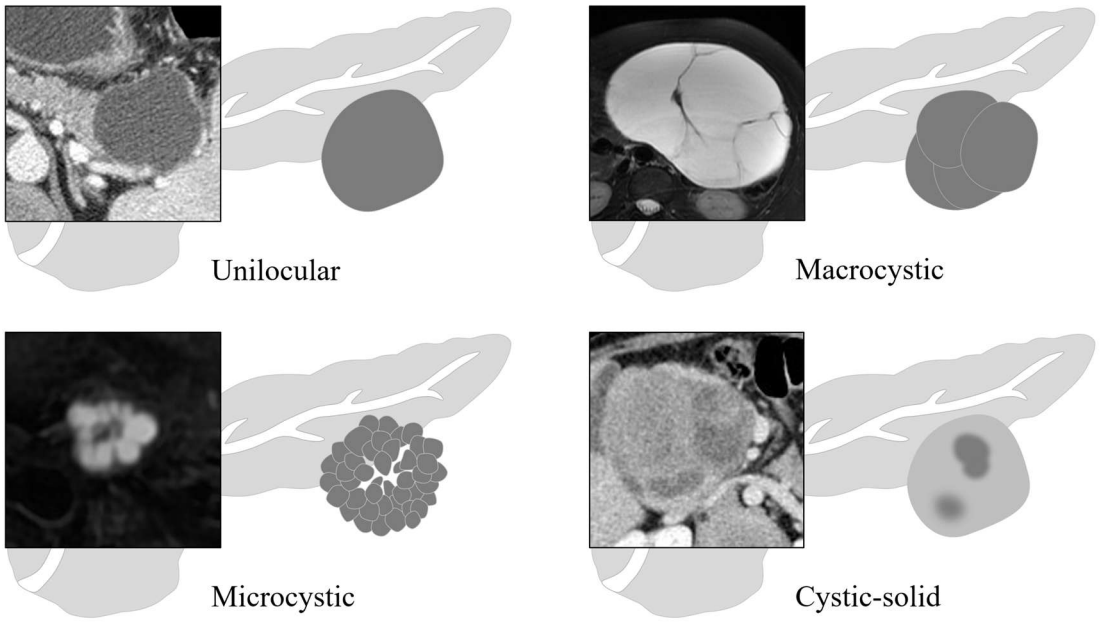


Figure S1. Schematic depicting representatives of morphology.

- **Unilocular**: a single fluid-filled cavity without any identifiable internal septa.
- **Macrocystic**: a lesion composed of multiple cysts, the largest of which measures ≥ 2 cm in diameter.
- **Microcystic**: a lesion composed of multiple cysts, the largest of which measures < 2 cm in diameter.
- **Cystic-solid**: a lesion that contains both a definite cystic portion and an independent solid component occupying > 50 of the total lesion volume.

For lesions with solid components in this study, the volumetric proportion of solid tissue was assessed using the most complete axial, coronal, and sagittal post□contrast images. Lesions were classified as "cystic□solid" if the solid component exceeded 50□ of the total lesion volume on at least two imaging planes. Otherwise, the primary cystic morphology—whether unilocular, macrocystic, or microcystic—

was retained and annotated as “with mural nodule.” A mural nodule is typically seen as a localized, papillary, or nodular solid projection arising from the cyst wall or a septation.

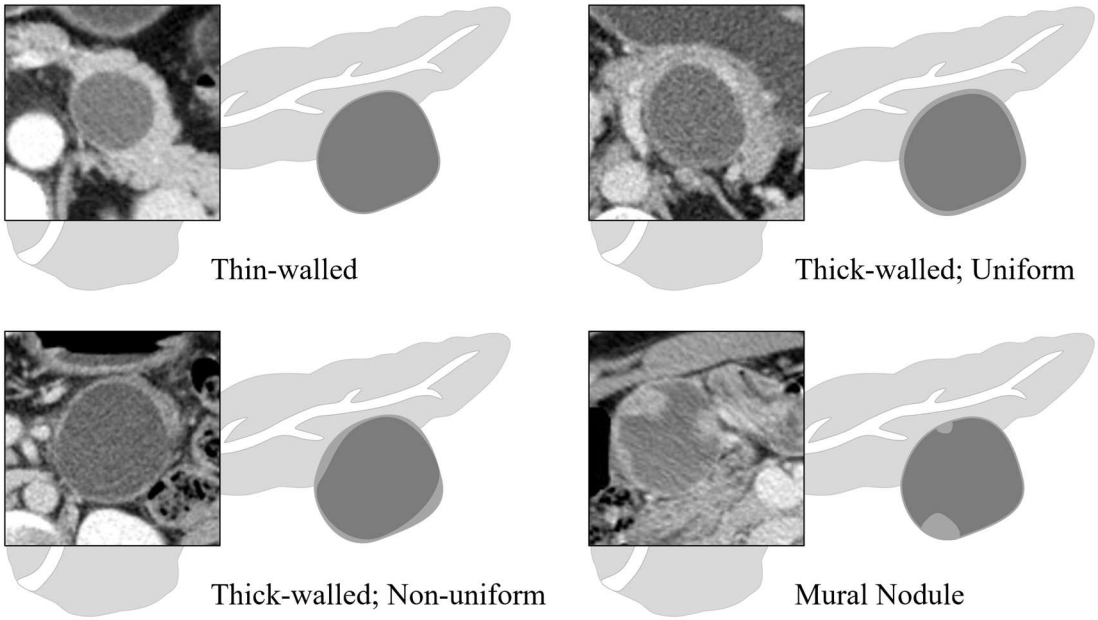

Figure S2. Schematic depicting representatives of cyst wall.

**Cyst Wall Thickness**

- Thin-walled (<2 mm)
- Thick-walled (≥2 mm)

On the axial post-contrast image that best delineates the cyst wall, the maximum wall thickness was measured along a straight segment, deliberately avoiding septal convergence points and mural nodule areas. Lesions were then classified into two categories: thick-walled (maximum thickness ≥ 2 mm) and thin-walled (maximum thickness < 2 mm). In polycystic lesions, the greatest wall thickness recorded among all locules was used for final assignment.

**Cyst Wall Uniformity**

- Uniform
- Non-uniform

Uniform: The cyst wall shows gradual thickness variation, with an inner margin

that is smooth and continuous, devoid of focal abrupt changes. Non-uniform: The wall thickness changes progressively, producing a “wavy” inner contour without giving rise to a discrete, measurable mural nodule. In polycystic lesions, if any single locule is judged to have a non-uniform wall, the entire lesion is recorded as having a non-uniform cyst wall.

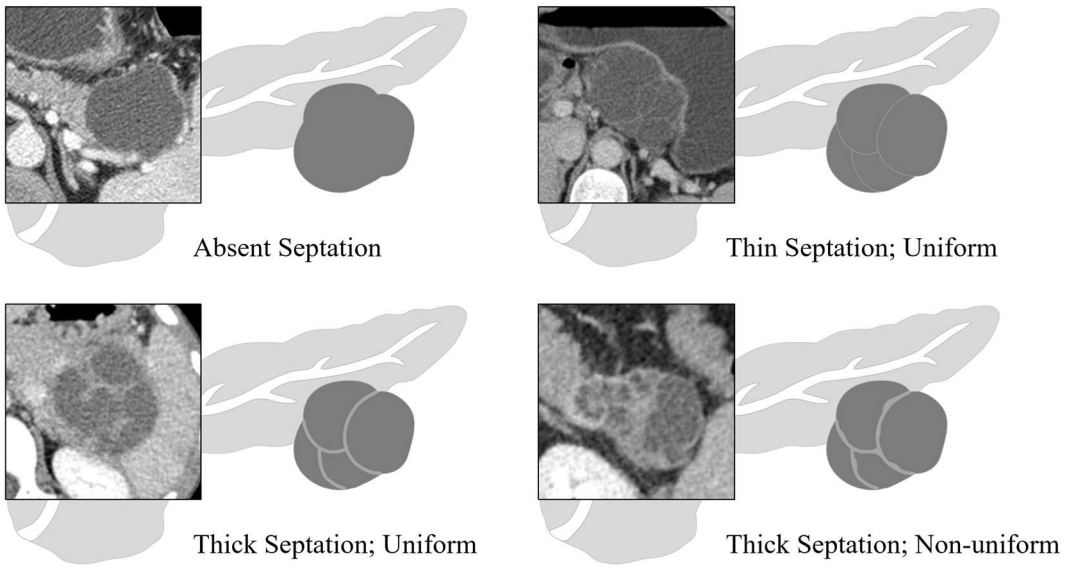


Figure S3. Schematic depicting representatives of septation.

**Septation Thickness**

- **Thin Septation:** maximum thickness < 2 mm.
- **Thick Septation**: maximum thickness ≥ 2 mm.

In this study, a septum is defined as a discernible, continuous linear structure traversing the cystic lumen and tethering the opposing cyst walls. On the post-contrast axial plane that most clearly delineates the septal architecture, the maximum thickness is measured perpendicularly at the straightest segment. When multiple septa are present, the greatest thickness recorded among all septa serves as the definitive value for classification.

**Septation Uniformity**

- **Uniform**: The septal thickness changes gradually, is smooth and continuous, and shows no focal abrupt alterations.
- **Non-uniform:** The septal thickness changes progressively, with the entire

septum or focal areas exhibiting a “beaded” appearance.

In multiple septated lesions, if any single septum is judged non-uniform, the septation of the entire lesion is recorded as non-uniform.

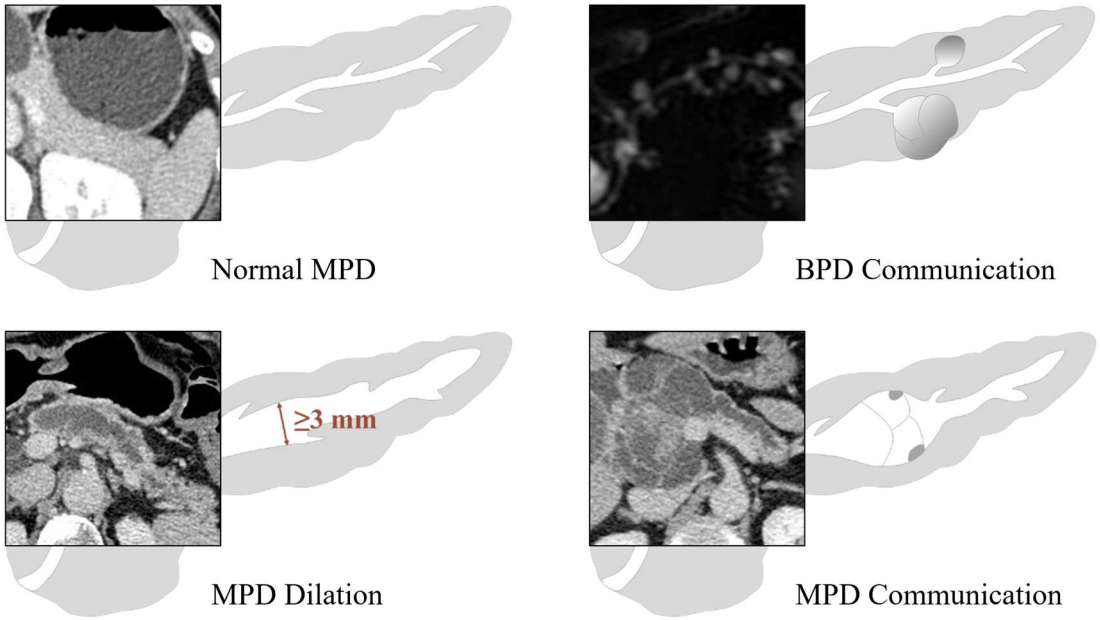


Figure S4. Schematic depicting representatives of pancreatic duct.

- **MPD Dilation:** Pancreatic duct dilation is defined as a focal or diffuse pathologic widening of the main pancreatic duct (MPD). On axial images, the widest intraparenchymal MPD diameter is measured; < 3 mm is recorded as "no dilation," ≥ 3 mm as "dilation." This assessment refers only to MPD caliber; side-branch morphology and communication with the lesion are not considered.

- **PD Communication:** Communication: A definite continuity between the lesion and the pancreatic duct is visible, or the lesion shows the classic "grape-cluster" appearance of dilated side branches. No communication: No such continuity is identified; pancreatic parenchyma separates the lesion from the duct.

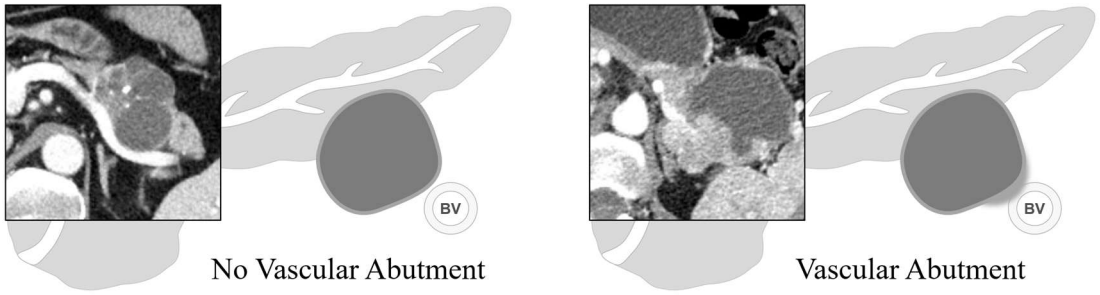


Figure S5. Schematic depicting representatives of vascular abutment.

Assessment of the relationship between the lesion and adjacent critical vessels (celiac trunk, superior mesenteric artery/vein, portal venous system, etc.).

- **No vascular abutment:** A clear fat plane or normal pancreatic parenchyma is interposed between the lesion and the vessel, or the lesion merely abuts the vessel without alteration of its contour, caliber, or wall smoothness.

- **Vascular abutment:** The lesion directly contacts the vessel with loss of the intervening fat plane or normal pancreatic parenchyma, or there is alteration of the vessel's contour, caliber, or wall smoothness.

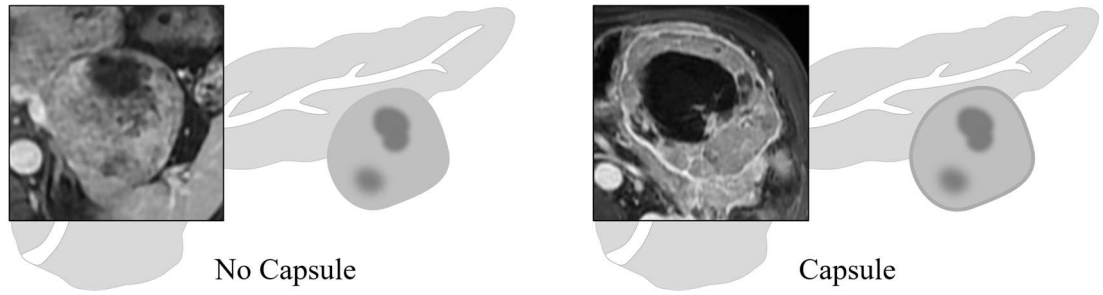


Figure S6. Schematic depicting representatives of capsule.

- **Capsule:** a complete, circumferential ring located at the outermost margin of the lesion that separates it from the surrounding normal pancreatic parenchyma. It typically appears as a hypodense/hypointense rim on unenhanced CT or T2WI and shows no or only minimal enhancement after contrast administration.

Figure S7. Schematic depicting representatives of pancreatic parenchymal atrophy.

- **Pancreatic parenchymal atrophy:** Diffuse or focal reduction in pancreatic parenchymal volume with irregular, serrated margins.

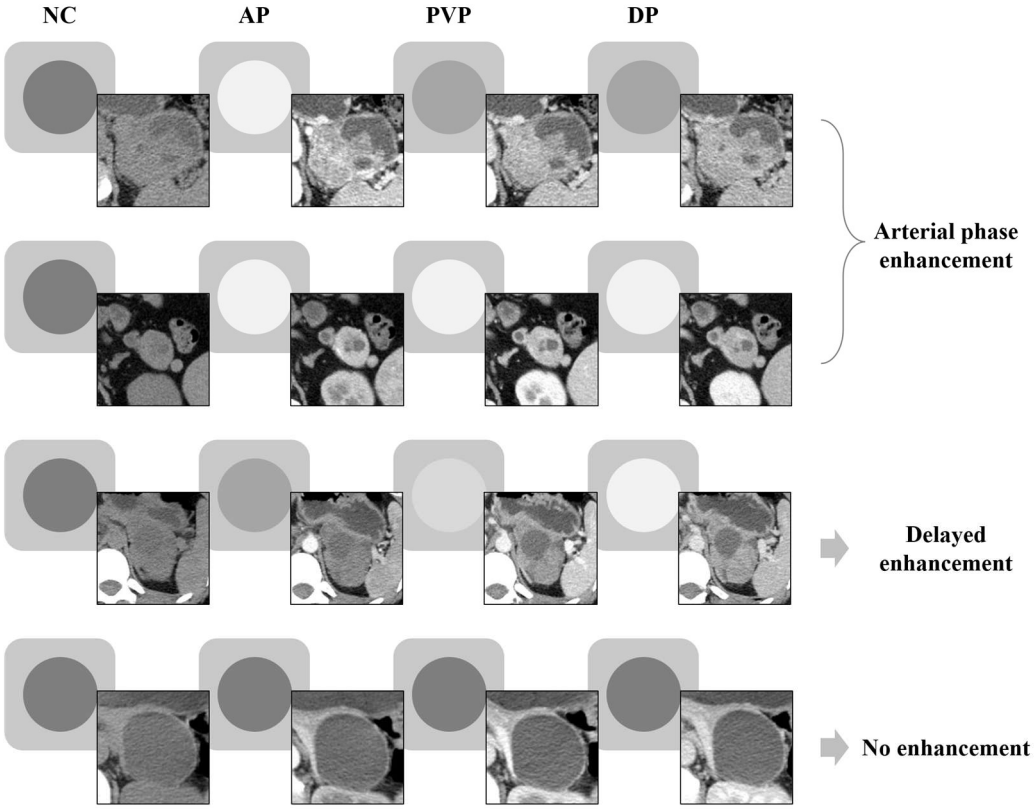

Figure S8. Schematic depicting representatives of enhancement.

- **No enhancement**: No perceptible change in CT attenuation or MRI signal intensity between the unenhanced and any post-contrast phase.

- **Arterial-phase enhancement**: A definite and marked increase in CT attenuation or MRI signal intensity is seen in the arterial phase, exceeding that of the surrounding normal pancreatic parenchyma, followed by persistent wash-out, plateau, or further enhancement on portal-venous and delayed phases.

- **Delayed enhancement**: No or only minimal enhancement in the arterial phase, with a progressive, gradual increase in enhancement on portal-venous and delayed phases, typically peaking on the delayed phase.

On contrast-enhanced CT or MRI, the enhancement pattern of the cyst wall, mural nodule, septa, and solid component was assessed separately.

## Appendix 2. Data processing, feature selection, and study size

### *2.1 Data processing and inter-rater reliability assessment*

#### 2.1.1 Data processing

Twenty categorical imaging variables that are device-independent and not specific to any particular imaging modality were evaluated: Lesion morphology, lesion location, lesion number, capsule, common bile duct dilation, cyst wall enhancement, cyst wall thickness, enlarged lymph nodes, intracystic septa enhancement, intracystic septations, main pancreatic duct (MPD) dilation, pancreatic duct (PD) communication, mural nodule enhancement, mural nodule in mpd, mural nodule status, pancreatic parenchymal atrophy, solid component enhancement,uniform cyst wall, uniform septations, vascular abutment. Nine continuous variables were also assessed: lesion dimensions, mural nodule and solid component dimensions, and main pancreatic and common bile duct diameters. Two patient demographics (age, sex), three clinical features (diabetes, jaundice, pancreatitis), and two tumour markers (serum CA 19-9 and CEA) were also recorded. Only variables with an overall missing rate below 15% were eligible for inclusion, and for categorical variables, each category was required to have a frequency greater than 10%. Clinical, radiological, and laboratory data were extracted from electronic medical records. Two abdominal radiologists independently reviewed all preoperative imaging, blinded to pathological results; a third radiologist resolved disagreements.

Prior to variable selection, inter-rater reliability was assessed among three radiologists: two junior radiologists (Radiologist A and Radiologist B, each with ≥5

years of experience in abdominal imaging) and one senior radiologist (Radiologist C, with >10 years of experience). All radiologists independently evaluated the imaging variables while blinded to each other's assessments and clinical outcomes.

2.1.2 Inter-rater reliability assessment

Inter-rater agreement was evaluated using pairwise comparisons among all three radiologists. The choice of statistical method was determined by the variable type and data distribution:

For categorical variables, Gwet's AC1 statistic was employed when data were sparse or exhibited prevalence-related bias, as it provides more stable estimates under conditions of high agreement with skewed marginal distributions. Cohen's kappa coefficient was used when the contingency table was adequately populated.

For continuous variables, Lin's concordance correlation coefficient (CCC) was calculated when normality assumptions were violated, providing a robust measure of agreement that accounts for both precision and accuracy. Intraclass correlation coefficient (ICC; two-way random effects model, absolute agreement, average measures) was calculated when both variables satisfied normality assumptions (Shapiro-Wilk test $P>0.05$).

Variables meeting the following thresholds in at least one pairwise comparison were retained for subsequent analysis: CCC or ICC >0.85 for continuous variables, and kappa or Gwet's AC1 >0.75 for categorical variables.

Table S2 presents the inter-rater reliability results for all 29 assessed imaging variables. All variables demonstrated acceptable agreement and were retained for

subsequent analysis. Agreement coefficients ranged from 0.598 to 0.998 across all pairwise comparisons.

Table S2 Inter-rater reliability coefficients for imaging variables assessed by three radiologists.

| Variable | Method | Junior A vs Senior | Junior B vs Senior |
|---|---|---|---|
| ***Continuous Variables*** | | | |
| Diameter of CBD (mm) | CCC | 0.925 | 0.878 |
| Diameter of MPD (mm) | CCC | 0.966 | 0.960 |
| Long diameter of largest mural nodule (mm) | CCC | 0.598 | 0.925 |
| Long diameter of lesion (mm) | CCC | 0.996 | 0.995 |
| Long diameter of solid component (mm) | CCC | 0.952 | 0.906 |
| Short diameter of largest lymph node (mm) | CCC | 0.740 | 0.910 |
| Short diameter of largest mural nodule (mm) | CCC | 0.781 | 0.916 |
| Short diameter of lesion (mm) | CCC | 0.993 | 0.992 |
| Short diameter of solid component (mm) | CCC | 0.941 | 0.969 |
| ***Categorical Variables*** | | | |
| Capsule | Gwet's AC1 | 0.948 | 0.932 |
| Common bile duct dilation | Gwet's AC1 | 0.983 | 0.967 |
| Cyst wall enhancement | Gwet's AC1 | 0.762 | 0.786 |
| Cyst wall thickness | Gwet's AC1 | 0.850 | 0.867 |
| Enlarged lymph nodes | Gwet's AC1 | 0.985 | 0.991 |
| Intracystic septation enhancement | Gwet's AC1 | 0.857 | 0.756 |
| Intracystic septations | Gwet's AC1 | 0.885 | 0.680 |
| Lesion location | Gwet's AC1 | 0.840 | 0.759 |
| Lesion number (single, multiple) | Gwet's AC1 | 0.976 | 0.976 |
| Lesion morphology | Gwet's AC1 | 0.790 | 0.783 |
| MPD dilation | Gwet's AC1 | 0.917 | 0.867 |
| PD communication | Gwet's AC1 | 0.887 | 0.840 |
| Mural nodule enhancement | Gwet's AC1 | 0.960 | 0.994 |
| Mural nodule in MPD | Gwet's AC1 | 0.998 | 0.993 |
| Mural nodule status | Gwet's AC1 | 0.963 | 0.995 |
| Pancreatic parenchymal atrophy | Gwet's AC1 | 0.963 | 0.884 |
| Solid component enhancement | Gwet's AC1 | 0.863 | 0.825 |
| Uniform cyst wall | Gwet's AC1 | 0.797 | 0.841 |
| Uniform septations | Gwet's AC1 | 0.761 | 0.694 |
| Vascular abutment | Gwet's AC1 | 0.871 | 0.778 |

**Abbreviations**: CCC, Lin's concordance correlation coefficient; ICC, intraclass correlation coefficient. Values represent agreement coefficients between junior radiologists (A or B) and the senior radiologist (C). Variables were retained if at least one pairwise comparison exceeded the threshold (>0.85 for continuous variables; >0.75 for categorical variables).

*2.2 Handling of missing data: multiple imputation*

Missing values were addressed using multiple imputation by chained equations (MICE; m = 10). The imputation procedure included CEA, CA19-9, jaundice, and diabetes, whereas pathological subtype and pathological risk outcomes were not included. MICE was performed separately in the development and temporal validation cohorts using the same prespecified procedure. Missingness for CEA and CA19-9 was 14.9% and 14.7%, respectively, in the development cohort and 13.3% for both variables in the temporal validation cohort. Predictive mean matching (PMM) was used for continuous laboratory variables.

To validate the imputation model, we compared the probability density distributions of the observed and imputed data. Visual inspection of the kernel density plots confirmed that the imputed values closely matched the distribution of the observed data, indicating that the imputation process preserved the original data structure without introducing significant distributional bias. In Figure S9-S10, the blue lines represent the density distribution of the original observed values for CEA and CA 19-9, while the red lines represent the distributions of the multiple imputed datasets generated by the MICE algorithm. The visual overlap indicates that the imputation process preserved the original data distribution structure without introducing significant bias (m=10).

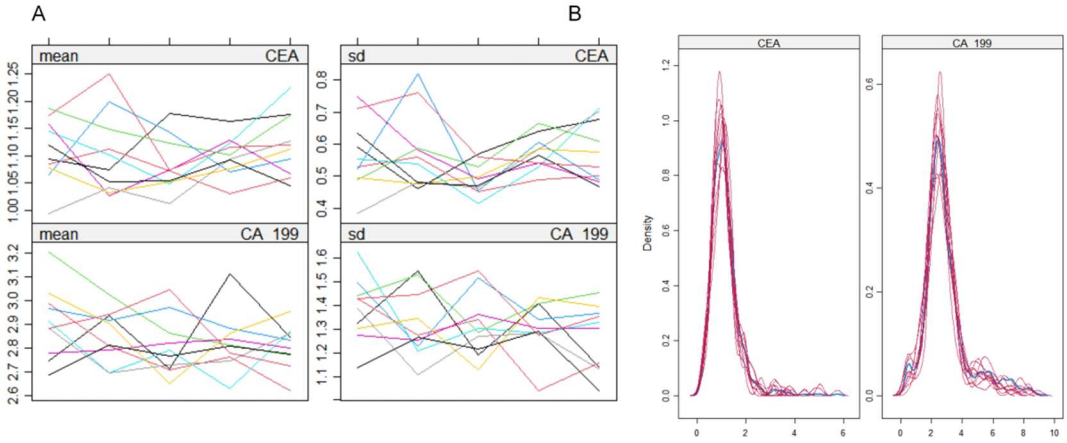


Figure S9. Density plots comparing the distribution of observed and imputed data for model development. (A) plots of mean and SD for CEA and CA19-9; (B) imputation of missing CEA and CA19-9.

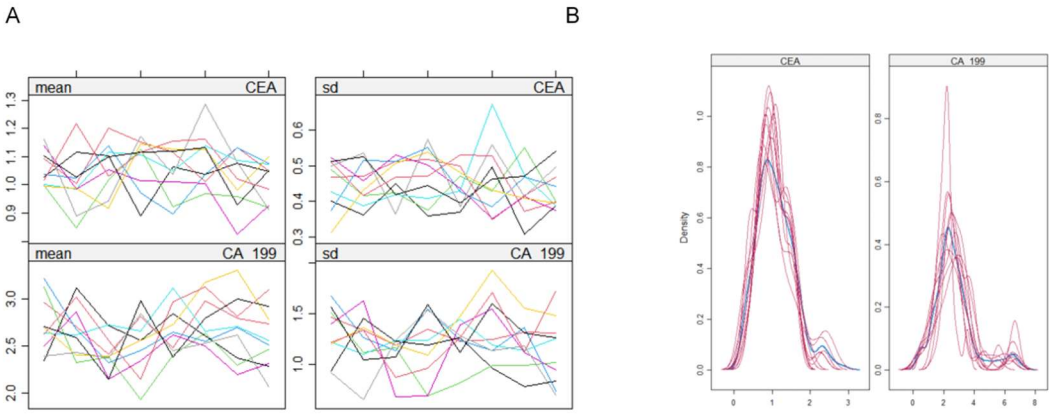


Figure S10. Density plots comparing the distribution of observed and imputed data for temporal validation. (A) plots of mean and SD for CEA and CA19-9; (B) imputation of missing CEA and CA19-9.

*2.3 Feature selection*

There were three criteria for feature selection. First, only variables with an overall missing rate below 15% were eligible for inclusion, and for categorical variables, each category was required to have a frequency greater than 10%.

Second, inter-rater reliability among radiologists was assessed to quantify measurement consistency (Table S3). A two-stage feature selection strategy was then applied to identify the most informative predictors while minimising overfitting, imputation uncertainty, and method-specific selection bias. In the first stage, highly correlated predictors (Pearson correlation coefficient >0.9) were identified and filtered to mitigate multicollinearity. When two or more variables were highly correlated, clinical expertise was used to retain the most clinically relevant or reliable variable.

In the second stage, feature selection was performed across the ten imputed datasets using a multi-method ensemble approach. Candidate predictors were independently screened using recursive feature elimination with cross-validation, tree-based feature importance, and L1-regularised regression, and were retained if selected by at least two methods. Selection frequencies were aggregated across the ten imputed datasets, and predictors selected in at least eight imputations ($\geqslant$ 80% selection frequency) were included in the final models (Supplementary Table 2.2). We also included the correspondence between the selected features and the guideline-defined worrisome features in Table S4.

Table S3. Predictors included in the model development

| Predictor | Categorisation | Five category model | IPMN risk model | MCN risk model |
|---|---|---|---|---|
| Sex | Categorical | Included | excluded | excluded |
| Age | Continuous | Included | excluded | Included |
| Long diameter of lesion (mm) | Continuous | Included | Included | excluded |
| Short diameter of lesion (mm) | Continuous | excluded | excluded | excluded |
| Long diameter of solid component (mm) | Continuous | excluded | excluded | excluded |
| Short diameter of solid component (mm) | Continuous | excluded | excluded | Included |
| Cyst wall thickness | Categorical | Included | Included | excluded |
| Uniform Cyst wall | Categorical | Included | Included | Included |
| Cyst wall enhancement | Categorical | Included | Included | Included |
| Mural nodule status | Categorical | excluded | excluded | excluded |
| Long diameter of largest mural nodule (mm) | Continuous | excluded | excluded | excluded |
| Short diameter of largest mural nodule (mm) | Continuous | excluded | excluded | Included |
| Mural nodule enhancement | Categorical | excluded | excluded | excluded |
| Solid component enhancement | Categorical | Included | excluded | excluded |
| Intracystic septations | Categorical | Included | excluded | excluded |
| Uniform Septations | Categorical | excluded | Included | excluded |
| Intracystic septa enhancement | Categorical | excluded | excluded | excluded |
| Capsule | Categorical | Included | excluded | excluded |
| PD communication | Categorical | Included | excluded | excluded |
| Pancreatic parenchymal atrophy | Categorical | Included | excluded | excluded |
| MPD dilation | Categorical | Included | excluded | excluded |
| Diameter of MPD (mm) | Continuous | excluded | Included | excluded |
| Mural nodule in MPD | Categorical | excluded | excluded | excluded |
| Common bile duct dilation | Categorical | excluded | excluded | excluded |
| Diameter of CBD (mm) | Continuous | excluded | excluded | excluded |
| Vascular abutment | Categorical | Included | Included | Included |
| Enlarged lymph nodes | Categorical | excluded | excluded | excluded |
| Short diameter of largest lymph node (mm) | Continuous | excluded | excluded | excluded |
| Lesion morphology | Categorical | Included | excluded | Included |
| Lesion_head_neck | Categorical | Included | excluded | excluded |
| Lesion_body_tail | Categorical | excluded | excluded | Included |
| Diabetes | Categorical | excluded | excluded | Included |
| Jaundice | Categorical | excluded | excluded | excluded |
| Pancreatis | Categorical | excluded | excluded | excluded |
| CA-199 | Continuous | Included | Included | excluded |
| CEA | Continuous | Included | Included | excluded |

Table S4. The indicators selected by four guidelines

| Grade classification | Indicators | ESG | Kyoto | HK | ACG* |
|---|---|---|---|---|---|
| High risk: the surgical management | Jaundice | √ | | √ | |
| | Jaundice with cystic lesion of the head of the pancreas | | √ | | |
| | Enhancing mural nodule>5 | √ | √ | √ | |
| | Solid mass | √ | √ | √ | |
| | MPD>10 | √ | √ | √ | |
| Medium risk: surveillance | enhancing or thick cyst walls | | √ | | |
| | CA19-9>37 | √ | √ | √ | √ |
| | Solid mass | | | | √ |
| | mural nodule | | | | √ |
| | enhancing mural nodule<5 | √ | √ | | |
| | mural nodule<5 | | | √ | |
| | MPD dilation | | | | √ |
| | MPD>5 | | | | √ |
| | 5<=MPD<9.9 | √ | √ | √ | √ |
| | Diabetes | √ | √ | √ | √ |
| | lymphadenopathy | | √ | | |
| | Pancreatitis | √ | √ | √ | √ |
| | cyst diameter>=30 | | √ | √ | √ |
| | cyst diameter>40 | √ | | | |
| | Pancreatic parenchymal atrophy | | √ | | √ |
| | acute pancreatitis | √ | √ | | √ |
| | Jaundice with cystic lesion | | | | √ |

Abbreviations: ESG, the European Study Group on Cystic Tumors of the Pancreas; ACG, the American College of Gastroenterology; HK, Hongkong

*ACG classification: For the ACG guideline, a binary risk classification was applied. Patients meeting any ACG-defined concerning criteria were classified as high risk, whereas those without these features were classified as low risk. The ACG guideline does not define a separate intermediate-risk category. For performance evaluation, pathologically confirmed low- and intermediate-risk lesions were combined into the non-high-risk group, whereas high-risk lesions were evaluated separately.

*2.4 Sample size*

Sample size considerations were informed by established methodological recommendations for the development and validation of multivariable prediction models with multinomial outcomes. The traditional rule of thumb requiring at least 10 events per variable (EPV) was considered as a historical reference rather than a definitive criterion for sample size adequacy. Given the unequal distribution of pathological categories, particular attention was paid to the number of patients in each outcome category and the complexity of the final prediction models. All eligible patients meeting the predefined inclusion criteria were included in the corresponding development and validation cohorts.

The development cohort comprised 858 patients, including 236 with IPMN (27.5%), 152 with MCN (17.7%), 281 with SCN (32.7%), 93 with SPN (10.8%), and 96 with NET (11.2%). Although the overall cohort provided representation of all five pathological subtypes, the relatively small numbers of SPN and NET cases may limit the precision and stability of class-specific predictions. To restrict model complexity and reduce the risk of overfitting, highly correlated predictors were removed, followed by a prespecified stability-based feature-selection procedure combining recursive feature elimination, tree-based feature importance, and L1-regularized regression.

Temporal validation cohort. The temporal validation cohort comprised 244 patients, including 78 with IPMN (32.0%), 33 with MCN (13.5%), 74 with SCN (30.3%), 41 with SPN (16.8%), and 18 with NET (7.4%). All eligible patients from the subsequent enrollment period (2023 – 2024) were included. Although this cohort enabled an independent temporal evaluation of model performance, the limited representation of uncommon pathological

subtypes, particularly NET, restricted the precision of class-specific performance estimates. Therefore, temporal validation was not considered equivalent to independent geographical or population-level temporal validation.

The IPMN development dataset included 236 patients, comprising 86 (36.4%) in the low-risk category, 41 (17.4%) in the intermediate-risk category, and 109 (46.2%) in the high-risk category. Nine predictors were retained in the final multinomial logistic regression model following the prespecified stability-based feature-selection procedure. Although the overall sample size supported model development, the smaller intermediate-risk category may have affected the stability of category-specific parameter estimates and prediction performance.

The MCN development dataset included 152 patients, comprising 109 (71.7%) in the low-risk category, 12 (7.9%) in the intermediate-risk category, and 31 (20.4%) in the high-risk category. Nine predictors were retained following correlation filtering and stability-based feature selection. The limited number of intermediate-risk cases was an important constraint on model development, and the conventional EPV heuristic could not establish sample size adequacy for this model. Five-fold cross-validation was employed to improve data utilization and assess internal model performance; however, neither cross-validation nor feature selection could compensate for the limited outcome information in the intermediate-risk category. Consequently, the stability and class-specific performance of the MCN model, particularly for intermediate-risk lesions, require cautious interpretation and further validation in larger independent cohorts.

No separate formal sample size calculation was performed for comparisons with guideline-based strategies or decision curve analysis. Instead, all eligible participants with the

required data from the temporal validation cohort were included in these analyses. Given the limited numbers of patients in certain pathological categories, findings from these secondary analyses were considered exploratory and interpreted in relation to the precision of the corresponding performance estimates.

*2.5 Decision curve analysis*

Four management strategies are applied: (1) diagnosis and risk stratification guided by the SIRS-PCL models; (2) real-world diagnosis of the same patients based on established clinical guidance. Net benefit was compared across four strategies: SIRS-PCL use, real-world radiologist assessment plus Hong Kong consensus use, and two reference strategies (treat all patients and treat no patients). Comparison of the SIRS-PCL with the Hong Kong consensus focused on three real-world perspectives: over-surgery (unnecessary resection of benign/low-risk lesions), over-examination (unwarranted invasive workup such as ESG for low-risk cases), and missed diagnosis (failure to identify high-risk malignancy).

## Appendix 3. Demographic tables for the three models

Appendix 3 presents the descriptive characteristics of the study populations used for the development and validation of all three models, including the five-category classification model, the IPMN risk stratification model, and the MCN risk stratification model.

Table S5. Descriptive statistics for patients in the entire cohort, including clinical and demographic characteristics

| Characteristic | Development cohort | | | | | | External verification cohort | | | | | |
|---|---|---|---|---|---|---|---|---|---|---|---|---|
| | Total | IPMN | MCN | NET | SCN | SPN | Total | IPMN | MCN | NET | SCN | SPN |
| | N = 858 | n = 236 | n = 152 | n = 96 | n = 281 | n = 93 | N = 244 | n = 78 | n = 33 | n = 18 | n = 74 | n = 41 |
| Female | 567 (66) | 95 (40) | 125 (82) | 51 (53) | 217 (77) | 79 (85) | 147 (60) | 31 (40) | 28 (85) | 5 (28) | 50 (68) | 33 (80) |
| Age | 55 [44, 64] | 63[56,67] | 55[41,62] | 54 [45, 59] | 55 [45, 63] | 29 [18, 39] | 58 [45,66] | 65 [58, 69] | 51 [40, 58] | 55 [40, 63] | 60 [52, 66] | 30 [22, 41] |
| Imaging modalities: | | | | | | | | | | | | |
| Contrast enhanced-CT | 590 (69) | 153 (65) | 113 (74) | 64 (67) | 197 (70) | 63 (68) | 166 (68) | 53 (68) | 29 (88) | 11 (61) | 49 (66) | 24 (59) |
| Contrast enhanced-MRI | 268 (31) | 83 (35) | 39 (26) | 32 (33) | 84 (30) | 30 (32) | 78 (32) | 25 (32) | 4 (12) | 7 (39) | 25 (34) | 17 (41) |
| Pathological risk stratification: | | | | | | | | | | | | |
| Benign | 313 (36) | 0 (0) | 49 (32) | 0 (0) | 264 (94) | 0 (0) | 70 (29) | 0 (0) | 9 (27) | 0 (0) | 61 (82) | 0 (0) |
| Low risk | 153 (18) | 86 (36) | 60 (39) | 0 (0) | 7 (2) | 0 (0) | 59 (24) | 30 (38) | 17 (52) | 0 (0) | 12 (16) | 0 (0) |
| Medium risk | 160 (19) | 41 (17) | 12 (8) | 30 (31) | 10 (4) | 67 (72) | 48 (20) | 9 (12) | 2 (6) | 5 (28) | 1 (1) | 31 (76) |
| High risk | 232 (27) | 109 (46) | 31 (20) | 66 (69) | 0 (0) | 26 (28) | 67 (27) | 39 (50) | 5 (15) | 13 (72) | 0 (0) | 10 (24) |
| Diabetes | | | | | | | | | | | | |
| Yes | 154 (18) | 56 (24) | 21 (14) | 20 (21) | 51 (18) | 6 (6) | 31 (13) | 18 (23) | 2 (6) | 0 (0) | 9 (12) | 2 (5) |
| No | 704 (82) | 180 (76) | 131 (86) | 76 (79) | 230 (82) | 87 (94) | 213 (87) | 60 (77) | 31 (94) | 18 (100) | 65 (88) | 39 (95) |
| Jaundice | | | | | | | | | | | | |
| Yes | 47 (5) | 19 (8) | 8 (5) | 6 (6) | 10 (4) | 4 (4) | 9 (4) | 6 (8) | 0 (0) | 1 (6) | 2 (3) | 0 (0) |
| No | 811 (95) | 217 (92) | 144 (95) | 90 (94) | 271 (96) | 89 (96) | 235 (96) | 72 (92) | 33 (100) | 17 (94) | 72 (97) | 41 (100) |

| Characteristic | Development cohort | | | | | | External verification cohort | | | | | |
|---|---|---|---|---|---|---|---|---|---|---|---|---|
| | Total N = 858 | IPMN n = 236 | MCN n = 152 | NET n = 96 | SCN n = 281 | SPN n = 93 | Total N = 244 | IPMN n = 78 | MCN n = 33 | NET n = 18 | SCN n = 74 | SPN n = 41 |
| Pancreatis | | | | | | | | | | | | |
| Yes | 23 (3) | 13 (6) | 5 (3) | 3 (3) | 1 (0) | 1 (1) | 3 (1) | 2 (3) | 1 (3) | 0 (0) | 0 (0) | 0 (0) |
| No | 835 (97) | 223 (94) | 147 (97) | 93 (97) | 280 (100) | 92 (99) | 241 (99) | 76 (97) | 32 (97) | 18 (100) | 74 (100) | 41 (100) |
| CA-199 (U/mL) | 12.6 [7.2, 27.5] | 19.6 [10.3, 83.8] | 14.1 [7.4, 39.1] | 14.1 [8.0, 31.6] | 10.6 [6.2, 17.9] | 9.8 [5.9, 14.0] | 11.0 [6.2, 21.6] | 18.2 [8.7, 71.3] | 9.2 [6.4, 17.5] | 17.1 [6.9, 25.8] | 8.5 [4.9, 11.6] | 8.6 [4.1, 17.7] |
| CEA (ng/mL) | 1.9 [1.2, 3.0] | 2.8 [1.8, 4.0] | 1.9 [1.0, 3.1] | 1.8 [1.4, 2.7] | 1.7 [1.2, 2.3] | 1.1 [0.7,1.7] | 1.8 [1.2, 3.1] | 2.7 [1.9, 4.1] | 1.8 [1.0, 3.8] | 2.1 [0.9, 2.6] | 1.6 [1.2, 2.5] | 1.1 [0.6, 1.5] |
| Lesion location [a]: | | | | | | | | | | | | |
| Pancreatic head/neck | 370 (43) | 150 (64) | 40 (26) | 49 (51) | 97 (35) | 34 (37) | 87 (36) | 44 (56) | 2 (6) | 5 (28) | 19 (26) | 17 (41) |
| Pancreatic body/tail | 511 (60) | 95 (40) | 117 (77) | 50 (52) | 189 (67) | 60 (65) | 168 (69) | 40 (51) | 31 (94) | 13 (72) | 57 (77) | 27 (66) |
| Lesion morphology: | | | | | | | | | | | | |
| Cystic-solid | 267 (31) | 67 (28) | 20 (13) | 87 (91) | 21 (8) | 72 (77) | 77 (32) | 24 (31) | 2 (6) | 11 (61) | 6 (8) | 34 (83) |
| Macrocystic | 178 (21) | 54 (23) | 65 (43) | 3 (3) | 48 (17) | 8 (9) | 59 (24) | 25 (32) | 19 (58) | 3 (17) | 10 (14) | 2 (5) |
| Microcystic | 264 (31) | 67 (28) | 17 (11) | 3 (3) | 175 (62) | 2 (2) | 58 (24) | 15 (19) | 0 (0) | 2 (11) | 41 (55) | 0 (0) |
| Unilocular | 149 (17) | 48 (20) | 50 (33) | 3 (3) | 37 (13) | 11 (12) | 50 (20) | 14 (18) | 12 (36) | 2 (11) | 17 (23) | 5 (12) |
| Overall lesion size: (mm) | | | | | | | | | | | | |
| Long diameter | 38 [28, 54] | 33 [25,45] | 43 [31,54] | 41 [28, 61] | 36 [27, 50] | 58 [39,82] | 36 [26,52] | 32 [24, 41] | 44 [30, 78] | 36 [24, 46] | 35 [27, 49] | 54 [35, 86] |
| Short diameter | 30 [21, 44] | 23 [17, 33] | 34 [24, 47] | 32 [23,48] | 29 [21, 40] | 49 [33,71] | 28 [20, 40] | 24 [16,29] | 39 [23, 61] | 24 [22, 38] | 28 [20, 40] | 44 [26,69] |
| Cyst wall thickness: | | | | | | | | | | | | |
| Absent cyst wall | 267 (31) | 67 (28) | 20 (13) | 87 (91) | 21 (8) | 72 (77) | 77 (32) | 24 (31) | 1 (3) | 11 (61) | 6 (8) | 34 (83) |
| Thick walled | 74 (9) | 24 (10) | 20 (13) | 6 (6) | 12 (4) | 12 (13) | 17 (7) | 9 (12) | 5 (15) | 2 (11) | 1 (1) | 1 (2) |
| Thin walled | 517 (60) | 145 (61) | 112 (74) | 3 (3) | 248 (88) | 9 (10) | 150 (61) | 45 (58) | 27 (82) | 5 (28) | 67 (91) | 6 (15) |
| Uniform Cyst wall: | | | | | | | | | | | | |

| Characteristic | Development cohort | | | | | | External verification cohort | | | | | |
|---|---|---|---|---|---|---|---|---|---|---|---|---|
| | Total N = 858 | IPMN n = 236 | MCN n = 152 | NET n = 96 | SCN n = 281 | SPN n = 93 | Total N = 244 | IPMN n = 78 | MCN n = 33 | NET n = 18 | SCN n = 74 | SPN n = 41 |
| Absent cyst wall | 267 (31) | 67 (28) | 20 (13) | 87 (91) | 21 (8) | 72 (77) | 77 (32) | 24 (31) | 1 (3) | 11 (61) | 6 (8) | 34 (83) |
| No | 109 (13) | 47 (20) | 20 (13) | 3 (3) | 29 (10) | 10 (11) | 27 (11) | 9 (12) | 10 (30) | 3 (17) | 5 (7) | 1 (2) |
| Yes | 482 (56) | 122 (52) | 112 (74) | 6 (6) | 231 (82) | 11 (12) | 140 (57) | 45 (58) | 22 (67) | 4 (22) | 63 (85) | 6 (15) |
| Cyst wall enhancement: | | | | | | | | | | | | |
| Absent cyst wall | 267 (31) | 67 (28) | 20 (13) | 87 (91) | 21 (8) | 72 (77) | 77 (32) | 24 (31) | 1 (3) | 11 (61) | 6 (8) | 34 (83) |
| Arterial-phase enhancement | 34 (4) | 16 (7) | 2 (1) | 1 (1) | 15 (5) | 0 (0) | 14 (6) | 4 (5) | 1 (3) | 3 (17) | 6 (8) | 0 (0) |
| Delayed enhancement | 246 (29) | 46 (19) | 54 (36) | 6 (6) | 125 (44) | 15 (16) | 32 (13) | 7 (9) | 13 (39) | 3 (17) | 8 (11) | 2 (5) |
| No enhancement | 311 (36) | 107 (45) | 76 (50) | 2 (2) | 120 (43) | 6 (7) | 121 (50) | 43 (55) | 18 (55) | 1 (6) | 54 (73) | 5 (12) |
| Mural nodule | 65 (8) | 15 (6) | 19 (13) | 2 (2) | 22 (8) | 7 (8) | 9 (4) | 4 (5) | 3 (9) | 0 (0) | 2 (3) | 0 (0) |
| Mural nodule size: (mm) | | | | | | | | | | | | |
| Long diameter | 12 [9,16] | 14 [9,17] | 12 [10, 16] | 6 [5,8] | 11 [7, 15] | 23 [14, 30] | 9 [9, 13] | 9 [8, 10] | 17 [13, 19] | 10 [9, 10] | | |
| Short diameter | 9 [7, 15] | 10 [8, 13] | 8 [7, 14] | 8 [5,11] | 9 [5, 19] | 9 [8, 21] | 6 [6,7] | 6 [5, 6] | 15 [11,15] | 5 [5,5] | | |
| Mural nodule enhancement: | | | | | | | | | | | | |
| Absent mural nodule | 793 (92) | 221 (94) | 133 (88) | 94 (98) | 259 (92) | 86 (92) | 235 (96) | 74 (95) | 30 (91) | 18 (100) | 72 (97) | 41(100) |
| Arterial-phase enhancement | 10 (1) | 2 (1) | 2 (1) | 1 (1) | 4 (1) | 1 (1) | 6 (2) | 4 (5) | 1 (3) | 0 (0) | 1 (1) | 0 (0) |
| Delayed enhancement | 45 (5) | 11 (5) | 11 (7) | 1 (1) | 16 (6) | 6 (7) | 2 (1) | 0 (0) | 2 (6) | 0 (0) | 0 (0) | 0 (0) |
| No enhancement | 10 (1) | 2 (1) | 6 (4) | 0 (0) | 2 (1) | 0 (0) | 1 (0) | 0 (0) | 0 (0) | 0 (0) | 1 (1) | 0 (0) |
| Solid component size: (mm) | | | | | | | | | | | | |
| Long diameter | 37 [26,55] | 31 [26, 42] | 32[ 24, 40] | 35 [25, 55] | 38 [27, 55] | 47 [33, 71] | 35 [22, 51] | 22 [21, 34] | 43 [41, 44] | 41 [22, 53] | 36 [26, 43] | 44 [27, 77] |
| Short diameter | 28 [21,45] | 25 [19, 33] | 23 [20, | 29 [21, | 30 [21, | 38 [24, | 25 [17, 38] | 20 [16, 28] | 33 [29, | 23 [15, | 21 [17, | 32 [22, 51] |

| Characteristic | Development cohort | | | | | | External verification cohort | | | | | |
|---|---|---|---|---|---|---|---|---|---|---|---|---|
| | Total N = 858 | IPMN n = 236 | MCN n = 152 | NET n = 96 | SCN n = 281 | SPN n = 93 | Total N = 244 | IPMN n = 78 | MCN n = 33 | NET n = 18 | SCN n = 74 | SPN n = 41 |
| | | | 27] | 45] | 35] | 56] | | | 37] | 38] | 29] | |
| Solid component enhancement: | | | | | | | | | | | | |
| Absent solid component | 590 (69) | 169 (72) | 131 (86) | 9 (9) | 260 (93) | 21 (23) | 165 (68) | 52 (67) | 31 (94) | 7 (39) | 68 (92) | 7 (17) |
| Arterial-phase enhancement | 84 (10) | 6 (3) | 0 (0) | 61 (64) | 7 (3) | 10 (11) | 22 (9) | 3 (4) | 0 (0) | 11 (61) | 4 (5) | 4 (10) |
| Delayed enhancement | 184 (21) | 61 (26) | 21 (14) | 26 (27) | 14 (5) | 62 (67) | 57 (23) | 23 (29) | 2 (6) | 0 (0) | 2 (3) | 30 (73) |
| Intracystic septation: | | | | | | | | | | | | |
| Absent septation | 324 (38) | 102 (43) | 61 (40) | 66 (69) | 45 (16) | 50 (54) | 104 (43) | 30 (38) | 12 (36) | 11 (61) | 19 (26) | 32 (78) |
| Thick septation | 133 (16) | 23 (10) | 19 (13) | 25 (26) | 30 (11) | 36 (39) | 23 (9) | 12 (15) | 4 (12) | 2 (11) | 3 (4) | 2 (5) |
| Thin septation | 401 (47) | 111 (47) | 72 (47) | 5 (5) | 206 (73) | 7 (8) | 117 (48) | 36 (46) | 17 (52) | 5 (28) | 52 (70) | 7 (17) |
| Uniform Septation: | | | | | | | | | | | | |
| Absent septation | 324 (38) | 102 (43) | 61 (40) | 66 (69) | 45 (16) | 50 (54) | 104 (43) | 30 (38) | 12 (36) | 11 (61) | 19 (26) | 32 (78) |
| No | 184 (21) | 38 (16) | 23 (15) | 24 (25) | 65 (23) | 34 (37) | 45 (18) | 18 (23) | 8 (24) | 4 (22) | 12 (16) | 3 (7) |
| Yes | 350 (41) | 96 (41) | 68 (45) | 6 (6) | 171 (61) | 9 (10) | 95 (39) | 30 (38) | 13 (39) | 3 (17) | 43 (58) | 6 (15) |
| Intracystic septation enhancement: | | | | | | | | | | | | |
| Absent septation | 324 (38) | 102 (43) | 61 (40) | 66 (69) | 45 (16) | 50 (54) | 104 (43) | 30 (38) | 12 (36) | 11 (61) | 19 (26) | 32 (78) |
| Arterial-phase enhancement | 62 (7) | 13 (6) | 3 (2) | 9 (9) | 35 (12) | 2 (2) | 32 (13) | 6 (8) | 4 (12) | 5 (28) | 16 (22) | 1 (2) |
| Delayed enhancement | 356 (41) | 81 (34) | 68 (45) | 17 (18) | 157 (56) | 33 (35) | 83 (34) | 34 (44) | 13 (39) | 2 (11) | 27 (36) | 7 (17) |
| No enhancement | 116 (14) | 40 (17) | 20 (13) | 4 (4) | 44 (16) | 8 (9) | 25 (10) | 8 (10) | 4 (12) | 0 (0) | 12 (16) | 1 (2) |
| Capsule | | | | | | | | | | | | |
| Yes | 108 (13) | 10 (4) | 4 (3) | 33 (34) | 3 (1) | 58 (62) | 35 (14) | 2 (3) | 1 (3) | 5 (28) | 3 (4) | 24 (59) |

| Characteristic | Development cohort | | | | | | External verification cohort | | | | | |
|---|---|---|---|---|---|---|---|---|---|---|---|---|
| | Total | IPMN | MCN | NET | SCN | SPN | Total | IPMN | MCN | NET | SCN | SPN |
| | N = 858 | n = 236 | n = 152 | n = 96 | n = 281 | n = 93 | N = 244 | n = 78 | n = 33 | n = 18 | n = 74 | n = 41 |
| No | 750 (87) | 226 (96) | 148 (97) | 63 (66) | 278 (99) | 35 (38) | 209 (86) | 76 (97) | 32 (97) | 13 (72) | 71 (96) | 17 (41) |
| PD communication | | | | | | | | | | | | |
| Yes | 217 (25) | 175 (74) | 16 (11) | 1 (1) | 24 (9) | 1 (1) | 72 (30) | 63 (81) | 1 (3) | 0 (0) | 7 (10) | 1 (2) |
| No | 641 (75) | 61 (26) | 136 (89) | 95 (99) | 257 (91) | 92 (99) | 172 (70) | 15 (19) | 32 (97) | 18 (100) | 67 (90) | 40 (98) |
| MPD dilation | | | | | | | | | | | | |
| Yes | 251 (29) | 109 (46) | 41 (27) | 28 (29) | 62 (22) | 11 (12) | 62 (25) | 46 (59) | 2 (6) | 6 (33) | 8 (11) | 0 (0) |
| No | 607 (71) | 127 (54) | 111 (73) | 68 (71) | 219 (78) | 82 (88) | 182 (75) | 32 (41) | 31 (94) | 12 (67) | 66 (89) | 41 (100) |
| Diameter of MPD (mm) | 6 [4, 10] | 8 [5, 11] | 5 [4, 8] | 6 [5, 8] | 5 [4, 7] | 6 [5, 7] | 7 [5, 9] | 7 [5, 10] | 6 [6, 6] | 6 [6,7] | 6 [4,10] | |
| Mural nodule in MPD | | | | | | | | | | | | |
| Yes | 9 (1) | 7 (3) | 2 (1) | 0 (0) | 0 (0) | 0 (0) | 1 (0) | 1 (1) | 0 (0) | 0 (0) | 0 (0) | 0 (0) |
| No | 849 (99) | 229 (97) | 150 (99) | 96 (100) | 281 (100) | 93 (100) | 243 (99) | 77 (99) | 33 (100) | 18 (100) | 74 (100) | 41 (100) |
| CBD dilation | | | | | | | | | | | | |
| Yes | 4 (1) | 2 (1) | 1 (1) | 1 (1) | 0 (0) | 0 (0) | 0 (0) | 0 (0) | 0 (0) | 0 (0) | 0 (0) | 0 (0) |
| No | 854 (99) | 234 (99) | 151 (99) | 95 (99) | 281 (100) | 93 (100) | 244 (100) | 78 (100) | 33 (100) | 18 (100) | 74 (100) | 41 (100) |
| Diameter of CBD (mm) | 14 [12,19] | 14 [12, 17] | 19 [17, 20] | 8 [3, 14] | 7 [4, 15] | 7 [2,12] | 15 [12,19] | 16[13,21] | | 12 [12,12] | 16 [16,16] | |
| Pancreatic parenchymal atrophy | | | | | | | | | | | | |
| Yes | 170 (20) | 79 (33) | 20 (13) | 20 (21) | 39 (14) | 12 (13) | 37 (15) | 21 (27) | 4 (12) | 5 (28) | 3 (4) | 4 (10) |
| No | 688 (80) | 157 (67) | 132 (87) | 76 (79) | 242 (86) | 81 (87) | 207 (85) | 57 (73) | 29 (88) | 13 (72) | 71 (96) | 37 (90) |
| Vascular abutment | | | | | | | | | | | | |
| Yes | 265 (31) | 77 (33) | 45 (30) | 51 (53) | 52 (19) | 40 (43) | 76 (31) | 24 (31) | 11 (33) | 11 (61) | 12 (16) | 18 (44) |
| No | 593 (69) | 159 (67) | 107 (70) | 45 (47) | 229 (81) | 53 (57) | 168 (69) | 54 (69) | 22 (67) | 7 (39) | 62 (84) | 23 (56) |
| Enlarged lymph nodes | | | | | | | | | | | | |
| Yes | 28 (3) | 10 (4) | 2 (1) | 12 (13) | 2 (1) | 2 (2) | 2 (1) | 2 (3) | 0 (0) | 0 (0) | 0 (0) | 0 (0) |

| Characteristic | Development cohort | | | | | | External verification cohort | | | | | |
|---|---|---|---|---|---|---|---|---|---|---|---|---|
| | Total | IPMN | MCN | NET | SCN | SPN | Total | IPMN | MCN | NET | SCN | SPN |
| | N = 858 | n = 236 | n = 152 | n = 96 | n = 281 | n = 93 | N = 244 | n = 78 | n = 33 | n = 18 | n = 74 | n = 41 |
| No | 830 (97) | 226 (96) | 150 (99) | 84 (87) | 279 (99) | 91 (98) | 242 (99) | 76 (97) | 33 (100) | 18 (100) | 74 (100) | 41 (100) |
| Short diameter of largest lymph node (mm) | 13 [11, 15] | 12 [11, 13] | 14 [14, 15] | 14 [11, 16] | 15 [12, 16] | 12 [11, 13] | 10 [10, 10] | 10 [10, 10] | | | | |

[1]Median [Q1, Q3] for continuous variables; n (%) for categorical variables

patients could have lesions in more than one location. CBD, Common bile duct; MPD, Main pancreatic duct;

Table S6. Characteristic distribution between model development and temporal validation Datasets for IPMN.

| Characteristic | Training set | | | | Validation set | | | |
|---|---|---|---|---|---|---|---|---|
| | low risk, N = 86[1] | Medium risk, N = 41[1] | High risk, N = 109[1] | Total, N=236 | low risk, N = 30[1] | Medium risk, N = 9[1] | High risk, N = 39[1] | Total, N=78 |
| Gender | | | | | | | | |
| Female | 33 (38) | 13 (32) | 49 (45) | 95 (40) | 8 (27) | 4 (44) | 19 (49) | 31 (40) |
| Male | 53 (62) | 28 (68) | 60 (55) | 141 (60) | 22 (73) | 5 (56) | 20 (51) | 47 (60) |
| Age | 63 [56, 67] | 59 [52, 65] | 64 [57, 70] | 63 [56,67] | 63 [61,66] | 60 [59, 68] | 66 [56, 71] | 65 [58,69] |
| Imaging Modalities | | | | | | | | |
| CE-CT | 57 (66) | 29 (71) | 67 (61) | 153 (65) | 21 (70) | 5 (56) | 27 (69) | 53 (68) |
| CE-MRI | 29 (34) | 12 (29) | 42 (39) | 83 (35) | 9 (30) | 4 (44) | 12 (31) | 25 (32) |
| Long diameter of lesion (mm) | 27 [19, 34] | 32 [24, 37] | 40 [29, 57] | 33 [25, 45] | 31 [26, 40] | 31 [26, 35] | 33 [23, 44] | 32 [24, 41] |
| Short diameter of lesion (mm) | 19 [13, 23] | 20 [15, 26] | 30 [22, 42] | 23 [17, 33] | 24 [17, 29] | 19 [16, 23] | 24 [16, 30] | 24 [16, 29] |
| Long diameter of solid component (mm) | 28 [23, 34] | 25 [21, 30] | 33 [26, 45] | 31 [26, 42] | 21 [20, 21] | | 24 [21, 34] | 22 [21, 34] |
| Short diameter of solid component (mm) | 17 [13, 24] | 19 [16, 22] | 26 [20, 33] | 25 [19, 33] | 16 [14, 18] | | 21 [16, 28] | 20 [16, 28] |
| Cyst wall thickness | | | | | | | | |
| Absent cyst wall | 4 (5) | 4 (9.8) | 57 (52) | 65 (28) | 2 (6.7) | 0 (0) | 20 (51) | 22 (28) |
| Thick-walled | 0 (0) | 5 (12) | 20 (18) | 25 (11) | 2 (6.7) | 1 (11) | 7 (18) | 10 (13) |
| Thin-walled | 82 (95) | 32 (78) | 32 (29) | 144 (61) | 26 (87) | 8 (89) | 12 (31) | 46 (59) |
| Uniform Cyst wall | | | | | | | | |
| Absent cyst wall | 4 (4.7) | 4 (9.8) | 57 (52) | 65 (28) | 2 (6.7) | 0 (0) | 20 (51) | 22 (28) |
| No | 5 (5.8) | 12 (29) | 31 (28) | 48 (20) | 2 (6.7) | 3 (33) | 5 (13) | 10 (13) |
| Yes | 77 (90) | 25 (61) | 21 (19) | 123 (52) | 26 (87) | 6 (67) | 14 (36) | 46 (59) |
| Cyst wall enhancement | | | | | | | | |

| Characteristic | Training set | | | | Validation set | | | |
|---|---|---|---|---|---|---|---|---|
| | low risk, N = 86[1] | Medium risk, N = 41[1] | High risk, N = 109[1] | Total, N=236 | low risk, N = 30[1] | Medium risk, N = 9[1] | High risk, N = 39[1] | Total, N=78 |
| Absent cyst wall | 4 (5) | 4 (19) | 57 (52) | 65 (28) | 2 (7) | 0 (0) | 20 (5) | 22 (28) |
| Arterial Phase Enhancement | 4 (5) | 2 (5) | 10 (9) | 16 (7) | 1 (3) | 0 (0) | 3 (8) | 4 (5) |
| Delayed enhancement | 18 (21) | 9 (22) | 19 (18) | 46 (19) | 3 (10) | 2 (22) | 2 (5) | 7 (9) |
| No enhancement | 60 (70) | 26 (63) | 23 (21) | 109 (46) | 24 (80) | 7 (78) | 14 (36) | 45 (58) |
| Mural nodule status | 3 (4) | 2 (5) | 10 (9) | 15 (6) | 1 (3.3) | 1 (11) | 2 (5) | 4 (5) |
| Long diameter of largest mural nodule (mm) | 10 [9, 12] | 21 [19, 23] | 14 [8, 16] | 14 [9, 17] | 9 [9, 9] | 9 [9, 9] | 10 [9, 11] | 9 [8, 10] |
| Short diameter of largest mural nodule (mm) | 12 [9, 13] | 19 [17, 20] | 10 [8, 10] | 10 [8, 13] | 5 [5, 5] | 6 [6, 6] | 6 [6, 6] | 6 [5, 6] |
| Mural nodule enhancement | | | | | | | | |
| Arterial Phase Enhancement | 1 (1) | 0 (0) | 1 (1) | 2 (1) | 1 (3) | 1 (11) | 2 (5) | 4 |
| Delayed enhancement | 0 (0) | 2 (5) | 9 (8) | 11 (5) | 0 (0) | 0 (0) | 0 (0) | 0 |
| No enhancement | 2 (2) | 0 (0) | 0 (0) | 2 (1) | 0 (0) | 0 (0) | 0 (0) | 0 |
| No mural nodule | 83 (97) | 39 (95) | 99 (91) | 221 (94) | 29 (97) | 8 (89) | 37 (95) | 74 |
| Solid component enhancement | | | | | | | | |
| Absence of solid tissue | 82 (95) | 37 (90) | 50 (46) | 169 (72) | 28 (93) | 9 (100) | 15 (38) | 52 |
| Arterial Phase Enhancement | 1 (1.2) | 0 (0) | 5 (4.6) | 6 | 0 (0) | 0 (0) | 3 (7.7) | 3 |
| Delayed enhancement | 3 (3.5) | 4 (9.8) | 54 (50) | 61 | 2 (6.7) | 0 (0) | 21 (54) | 23 |
| Intracystic septations | | | | | | | | |
| Absent septations | 31 (36) | 10 (24) | 61 (56) | 102 | 6 (20) | 1 (11) | 23 (59) | 30 |
| Thick septations | 0 (0) | 5 (12) | 18 (17) | 23 | 3 (10) | 3 (33) | 6 (15) | 12 |
| Thin septations | 55 (64) | 26 (63) | 30 (28) | 111 | 21 (70) | 5 (56) | 10 (26) | 36 |
| Uniform Septations | | | | | | | | |

| Characteristic | Training set | | | | Validation set | | | |
|---|---|---|---|---|---|---|---|---|
| | low risk, N = 86[1] | Medium risk, N = 41[1] | High risk, N = 109[1] | Total, N=236 | low risk, N = 30[1] | Medium risk, N = 9[1] | High risk, N = 39[1] | Total, N=78 |
| Absent septations | 31 (36) | 10 (24) | 61 (56) | 102 | 6 (20) | 1 (11) | 23 (59) | 30 |
| No | 4 (4.7) | 7 (17) | 27 (25) | 38 | 5 (17) | 2 (22) | 11 (28) | 18 |
| Yes | 51 (59) | 24 (59) | 21 (19) | 96 | 19 (63) | 6 (67) | 5 (13) | 30 |
| Intracystic septa enhancement | | | | | | | | |
| Absent septations | 31 (36) | 10 (24) | 61 (56) | 102 | 6 (20) | 1 (11) | 23 (59) | 30 (38) |
| Arterial Phase Enhancement | 7 (8.1) | 0 (0) | 6 (5.5) | 13 | 1 (3.3) | 2 (22) | 3 (8) | 6 (8) |
| Delayed enhancement | 29 (34) | 20 (49) | 32 (29) | 81 | 16 (53) | 6 (67) | 12 (31) | 34 (44) |
| No enhancement | 19 (22) | 11 (27) | 10 (9.2) | 30 | 7 (23) | 0 (0) | 1 (2) | 8 (10) |
| Capsule | | | | | | | | |
| Yes | 0 (0) | 1 (2) | 9 (8) | 10 | 0 (0) | 0 (0) | 2 (5) | 2 (3) |
| No | 86 (100) | 40 (98) | 100 (92) | 226 | 30 (100) | 9 (100) | 37 (95) | 76 (97) |
| PD communication | | | | | | | | |
| Yes | 59 (69) | 35 (85) | 81 (74) | 175 (74) | 25 (83) | 8 (89) | 30 (77) | 63 (81) |
| No | 27 (21) | 6 (15) | 28 (26) | 61 (26) | 5 (17) | 1 (11) | 9 (23) | 15 (19) |
| Pancreatic parenchymal atrophy | | | | | | | | |
| Yes | 8 (9) | 12 (29) | 59 (54) | 79 (33) | 5 (17) | 1 (11) | 15 (38) | 21 |
| No | 78 (91) | 29 (71) | 50 (46) | 157 (67) | 25 (83) | 8 (89) | 24 (62) | 57 |
| MPD dilation | | | | | | | | |
| Yes | 39 (45) | 24 (59) | 46 (42) | 109 | 15 (50) | 6 (67) | 25 (64) | 46 |
| No | 47 | 17 | 63 | 127 | 15 | 3 | 14 | 32 |
| Diameter of MPD (mm) | 6 [4, 7] | 9 [6, 10] | 9 [6, 12] | 8 [5, 11] | 7 [5, 9] | 6 [5, 8] | 8 [5, 10] | 7 [5, 10] |
| Mural nodule in MPD | | | | | | | | |

| Characteristic | Training set | | | | Validation set | | | |
|---|---|---|---|---|---|---|---|---|
| | low risk, N = 86[1] | Medium risk, N = 41[1] | High risk, N = 109[1] | Total, N=236 | low risk, N = 30[1] | Medium risk, N = 9[1] | High risk, N = 39[1] | Total, N=78 |
| Yes | 0 (0) | 0 (0) | 7 (6.4) | 7 | 0 (0) | 0 (0) | 1 (2.6) | 1 |
| No | 86 | 41 | 102 | 229 | 30 | 9 | 38 | 77 |
| Common bile duct dilation | | | | | | | | |
| Yes | 1 (1.2) | 0 (0) | 1 (0.9) | 2 | 0 (0) | 0 (0) | 0 (0) | 0 |
| No | 85 | 41 | 108 | 234 | 30 | 9 | 39 | 78 |
| Diameter of CBD (mm) | 12 [11, 16] | | 14 [12,16] | 14 [12, 17] | 10 [10, 10] | | 18 [14, 21] | 16 [13, 21] |
| Vascular abutment | | | | | | | | |
| Yes | 5 (5.8) | 5 (12) | 67 (61) | 77 | 1 (3.3) | 1 (11) | 22 (56) | 24 |
| No | 81 | 36 | 42 | 159 | 29 | 8 | 17 | 54 |
| Enlarged lymph nodes | | | | | | | | |
| Yes | 1 (1.2) | 0 (0) | 9 (8.3) | 10 | 0 (0) | 0 (0) | 2 (5.1) | 2 |
| No | 85 | 41 | 100 | 226 | 30 | 9 | 37 | 76 |
| Short diameter of largest lymph node (mm) | 12 [11, 16] | | 14 [12, 16] | 12 [11, 13] | | | | 10 [10, 10] |
| Distant metastasis | | | | | | | | |
| Yes | 0 (0) | 1 (2) | 4 (4) | 5 | 0 (0) | 0 (0) | 1 (2.6) | 1 |
| No | 86 | 40 | 105 | 231 | 30 | 9 | 38 | 77 |
| Tumor lesion | | | | | | | | |
| Cystic-solid | 4 (4.7) | 4 (9.8) | 58 (53) | 66 | 2 (6.7) | 0 (0) | 22 (56) | 24 |
| Macrocystic | 25 (29) | 12 (29) | 18 (17) | 55 | 13 (43) | 4 (44) | 8 (21) | 25 |
| Microcystic | 30 (35) | 19 (46) | 19 (17) | 68 | 10 (33) | 4 (44) | 1 (2.6) | 15 |
| Unilocular | 27 (31) | 6 (15) | 14 (13) | 47 | 5 (17) | 1 (11) | 8 (21) | 14 |

| Characteristic | Training set | | | | Validation set | | | |
|---|---|---|---|---|---|---|---|---|
| | low risk, N = 86[1] | Medium risk, N = 41[1] | High risk, N = 109[1] | Total, N=236 | low risk, N = 30[1] | Medium risk, N = 9[1] | High risk, N = 39[1] | Total, N=78 |
| Lesion location | | | | | | | | |
| Head and neck | 48 (56) | 30 (73) | 72 (66) | 150 | 17 (57) | 7 (78) | 20 (51) | 44 |
| Body and tail | 39 (45) | 13 (32) | 43 (39) | 95 | 15 (50) | 4 (44) | 21 (54) | 40 |
| Diabetes | | | | | | | | |
| Yes | 6 (9.4) | 9 (24) | 41 (39) | 56 | 9 (36) | 1 (13) | 8 (21) | 18 |
| No | 80 | 32 | 68 | 180 | 5 | 1 | 1 | 7 |
| Jaundice | | | | | | | | |
| Yes | 1 (1.6) | 0 (0) | 18 (17) | 19 | 1 (4.2) | 0 (0) | 5 (13) | 6 |
| No | 85 | 41 | 91 | 217 | 29 | 9 | 34 | 72 |
| ln(CA 19-9 + 1) | 2.6 [2.2, 3.0] | 2.8 [2.2, 3.7] | 3.9 [2.7, 5.9] | 3.0 [2.4, 4.4] | 2.5 [2.2, 2.8] | 2.7 [2.1, 3.0] | 3.6 [2.7, 5.9] | 3.0 [2.3, 4.3] |
| ln(CEA + 1) | 1.1 [0.9, 1.5] | 1.4 [1.1, 1.7] | 1.4 [1.2, 1.8] | 1.3 [1.0, 1.6] | 1.3 [1.1, 1.4] | 1.4 [1.1, 1.7] | 1.5 [1.0, 1.8] | 1.3 [1.0, 1.6] |

[1]Median [Q1, Q3] for continuous variables; n (%) for categorical variables

[a] Not mutually exclusive; patients could have lesions in more than one location. SCN, serous cystadenoma; MCN, mucinous cystic neoplasm; IPMN, intraductal papillary mucinous neoplasm; SPN, solid pseudopapillary neoplasm; NET, neuroendocrine tumor; MPD, Main pancreatic duct; CBD, Common bile duct.

Note: Serum CA 19-9 and CEA concentrations were originally measured in U/mL and ng/mL, respectively. When log-transformed values are reported, the transformation is expressed as ln(CA 19-9 + 1) and ln(CEA + 1), respectively.

Table S7. Characteristic distribution between model development and temporal validation Datasets for MCN.

| Characteristic | Training set | | | | | Validation set | | | | |
|---|---|---|---|---|---|---|---|---|---|---|
| | Benign, N = 49[1] | Low risk, N = 60[1] | Medium risk, N = 12[1] | High risk, N = 31[1] | Total, N=152 | Benign, N = 9[1] | Low risk, N = 17[1] | Medium risk, N = 2[1] | High risk, N = 5[1] | Total, N=33 |
| Gender | | | | | | | | | | |
| Female | 44 | 53 | 10 | 18 | 125 | 7 | 15 | 2 | 4 | 28 |
| Male | 5 | 7 | 2 | 13 | 27 | 2 | 2 | 0 | 1 | 5 |
| Age | 49 [36, 59] | 51 [40, 61] | 62 [37, 69] | 59 [56, 70] | 55 [41,62] | 45 [40, 58] | 51[38, 57] | 50 [42, 58] | 51 [47, 53] | 51 [40, 58] |
| Imaging Modalities | | | | | | | | | | |
| CE-CT | 38 | 46 | 6 | 23 | 113 | 8 | 14 | 2 | 5 | 29 |
| CE-MRI | 11 | 14 | 6 | 8 | 39 | 1 | 3 | 0 | 0 | 4 |
| Tumor lesion | | | | | | | | | | |
| Cystic-solid | 1 | 3 | 0 | 16 | 20 | 0 | 1 | 0 | 1 | 2 |
| Macrocystic | 22 | 25 | 9 | 9 | 65 | 5 | 8 | 2 | 4 | 19 |
| Microcystic | 4 | 7 | 2 | 4 | 17 | 0 | 0 | 0 | 0 | 0 |
| Unilocular | 22 | 25 | 1 | 2 | 50 | 4 | 8 | 0 | 0 | 12 |
| Long diameter of lesion (mm) | 44 [31, 53] | 38 [31, 53] | 48 [27, 59] | 44 [30, 60] | 43 [31, 54] | 30 [26, 78] | 40 [30, 61] | 121 [107, 135] | 77 [60, 104] | 44 [30, 78] |
| Short diameter of lesion (mm) | 38 [25, 47] | 32 [23, 46] | 38 [20, 52] | 35 [28, 48] | 34 [24, 47] | 23 [18,53] | 35 [26, 46] | 110 [95, 125] | 62 [53, 70] | 39 [23, 61] |
| Long diameter of solid component (mm) | 27 [27, 27] | 40 [40, 40] | - | 30 [22, 35] | 32 [24, 40] | - | 46 [46, 46] | - | 40 [40, 40] | 43 [41, 44] |
| Short diameter of solid component (mm) | 23 [23, 23] | 24 [23, 24] | - | 23 [20, 31] | 23 [20, 27] | - | 41 [41, 41] | - | 25 [25, 25] | 33 [29, 37] |
| Cyst wall thickness | | | | | | | | | | |
| Absent cyst wall | 1 | 3 | 0 | 16 | 20 | 0 | 1 | 0 | 0 | 1 |
| Thick-walled | 4 | 6 | 3 | 7 | 20 | 0 | 1 | 1 | 3 | 5 |
| Thin-walled | 44 | 51 | 9 | 8 | 112 | 9 | 15 | 1 | 2 | 27 |
| Uniform Cyst wall | | | | | | | | | | |
| Absent cyst wall | 1 | 3 | 0 | 16 | 20 | 0 | 1 | 0 | 0 | 1 |
| No | 3 | 1 | 5 | 11 | 20 | 0 | 3 | 2 | 5 | 10 |
| Yes | 45 | 56 | 7 | 4 | 112 | 9 | 13 | 0 | 0 | 22 |
| Cyst wall enhancement | | | | | | | | | | |
| Absent cyst wall | 1 | 3 | 0 | 16 | 20 | 0 | 1 | 0 | 0 | 1 |
| Arterial Phase Enhancement | 1 | 0 | 0 | 1 | 2 | 1 | 0 | 0 | 0 | 1 |
| Delayed enhancement | 13 | 21 | 8 | 12 | 54 | 0 | 6 | 2 | 5 | 13 |
| No enhancement | 34 | 36 | 4 | 2 | 76 | 8 | 10 | 0 | 0 | 18 |
| Mural nodule status | | | | | | | | | | |
| Yes | 6 | 7 | 0 | 6 | 19 | 0 | 1 | 0 | 2 | 3 |
| No | 43 | 53 | 12 | 25 | 133 | 9 | 16 | 2 | 3 | 30 |

| Characteristic | Training set | | | | | Validation set | | | | |
|---|---|---|---|---|---|---|---|---|---|---|
| | **Benign, N = 49[1]** | **Low risk, N = 60[1]** | **Medium risk, N = 12[1]** | **High risk, N = 31[1]** | **Total, N=152** | **Benign, N = 9[1]** | **Low risk, N = 17[1]** | **Medium risk, N = 2[1]** | **High risk, N = 5[1]** | **Total, N=33** |
| Long diameter of largest mural nodule (mm) | 11 [9, 13] | 12 [9, 14] | | 13 [11, 19] | 12 [10, 16] | - | 9 [9, 9] | - | 19 [18, 21] | 17 [13, 19] |
| Short diameter of largest mural nodule (mm) | 8 [6, 12] | 7 [6, 8] | | 14 [12, 15] | 8 [7, 14] | - | 7 [7, 7] | - | 15 [15,15] | 15 [11, 15] |
| Mural nodule enhancement | | | | | | | | | | |
| Arterial Phase Enhancement | 1 | 0 | 0 | 1 | 2 | 0 | 1 | 0 | 0 | 1 |
| Delayed enhancement | 3 | 4 | 0 | 4 | 11 | 0 | 0 | 0 | 2 | 2 |
| No enhancement | 2 | 3 | 0 | 1 | 6 | 0 | 0 | 0 | 0 | 0 |
| No mural nodule | 43 | 53 | 12 | 25 | 133 | 9 | 16 | 2 | 3 | 30 |
| Solid component enhancement | | | | | | | | | | |
| Absence of solid tissue | 48 | 57 | 12 | 14 | 131 | 9 | 16 | 2 | 4 | 31 |
| Arterial Phase Enhancement | 0 | 0 | 0 | 0 | 0 | 0 | 0 | 0 | 0 | 0 |
| Delayed enhancement | 1 | 3 | 0 | 17 | 21 | 0 | 1 | 0 | 1 | 2 |
| Intracystic septations | | | | | | | | | | |
| Absent septations | 22 | 27 | 1 | 11 | 61 | 4 | 8 | 0 | 0 | 12 |
| Thick septations | 1 | 4 | 2 | 12 | 19 | 0 | 1 | 1 | 2 | 4 |
| Thin septations | 26 | 29 | 9 | 8 | 72 | 5 | 8 | 1 | 3 | 17 |
| Uniform Septations | | | | | | | | | | |
| Absent septations | 22 | 27 | 1 | 11 | 61 | 4 | 8 | 0 | 0 | 12 |
| No | 4 | 5 | 1 | 13 | 23 | 0 | 2 | 2 | 4 | 8 |
| Yes | 23 | 28 | 10 | 7 | 68 | 5 | 7 | 0 | 1 | 13 |
| Intracystic septa enhancement | | | | | | | | | | |
| Absent septations | 22 | 27 | 1 | 11 | 61 | 4 | 8 | 0 | 0 | 12 |
| Arterial Phase Enhancement | 3 | 0 | 0 | 0 | 3 | 2 | 2 | 0 | 0 | 4 |
| Delayed enhancement | 19 | 22 | 7 | 20 | 68 | 2 | 5 | 2 | 4 | 13 |
| No enhancement | 5 | 11 | 4 | 0 | 20 | 1 | 2 | 0 | 1 | 4 |
| Capsule | | | | | | | | | | |
| Yes | 1 | 0 | 0 | 3 | 4 | 0 | 1 | 0 | 0 | 1 |
| No | 48 | 60 | 12 | 28 | 148 | 9 | 16 | 2 | 5 | 32 |
| Main PD communication | 4 | 6 | 1 | 5 | 16 | 1 | 0 | 0 | 0 | 1 |
| Pancreatic parenchymal atrophy | 5 | 6 | 1 | 8 | 20 | 0 | 1 | 0 | 3 | 4 |
| MPD dilation | 7 | 13 | 4 | 17 | 41 | 1 | 1 | 0 | 0 | 2 |

| Characteristic | Training set | | | | | Validation set | | | | |
|---|---|---|---|---|---|---|---|---|---|---|
| | Benign, N = 49[1] | Low risk, N = 60[1] | Medium risk, N = 12[1] | High risk, N = 31[1] | Total, N=152 | Benign, N = 9[1] | Low risk, N = 17[1] | Medium risk, N = 2[1] | High risk, N = 5[1] | Total, N=33 |
| Diameter of MPD (mm) | 4 [3, 6] | 6 [4, 7] | 7 [7, 7] | 5 [4, 8] | 5 [4, 8] | 6.4 [6.4, 6.4] | 6.1 [6.1, 6.1] | - | - | 6 [6, 6] |
| Mural nodule in MPD | | | | | | | | | | |
| Yes | 0 | 1 | 0 | 1 | 2 | 0 | 0 | 0 | 0 | 0 |
| No | 49 | 59 | 12 | 30 | 150 | 9 | 17 | 2 | 5 | 33 |
| Common bile duct dilation | | | | | | | | | | |
| Yes | 0 | 0 | 0 | 1 | 1 | 0 | 0 | 0 | 0 | 0 |
| No | 49 | 60 | 12 | 30 | 151 | 9 | 17 | 2 | 5 | 33 |
| Diameter of CBD (mm) | 14 [13, 15] | 20 [20, 20] | - | 19 [19, 21] | 19 [17, 20] | - | - | - | - | - |
| Vascular abutment | | | | | | | | | | |
| Yes | 8 | 10 | 6 | 21 | 45 | 0 | 4 | 2 | 5 | 11 |
| No | 41 | 50 | 6 | 10 | 107 | 9 | 13 | 0 | 0 | 22 |
| Enlarged lymph nodes | | | | | | | | | | |
| Yes | 1 | 1 | 0 | 0 | 2 | 0 | 0 | 0 | 0 | 0 |
| No | 48 | 59 | 12 | 31 | 150 | 9 | 17 | 2 | 5 | 33 |
| Short diameter of largest lymph node (mm) | 16 [16, 16] | 13 [13, 13] | | | 14 [14, 15] | - | - | - | - | - |
| Lesion location | | | | | | | | | | |
| Head and neck | 5 | 13 | 4 | 18 | 40 | 1 | 1 | 0 | 0 | 2 |
| Body and tail | 47 | 49 | 8 | 13 | 117 | 8 | 16 | 2 | 5 | 31 |
| Diabetes | | | | | | | | | | |
| Yes | 3 | 6 | 0 | 12 | 21 | 0 | 1 | 0 | 1 | 2 |
| No | 46 | 54 | 12 | 19 | 131 | 9 | 16 | 2 | 4 | 31 |
| Jaundice | | | | | | | | | | |
| Yes | 1 | 4 | 0 | 3 | 8 | 0 | 0 | 0 | 0 | 0 |
| No | 48 | 56 | 12 | 28 | 144 | 9 | 17 | 2 | 5 | 33 |
| ln(CA 19-9 + 1) | 2.3 [2.0, 3.1] | 2.7 [2.2, 3.4] | 3.1 [2.4, 3.3] | 4.9 [2.6, 5.4] | 2.7 [2.1, 3.7] | 2.1 [1.9, 2.5] | 2.2 [1.9, 2.6] | 2.9 [2.9, 2.9] | 4.1 [3.2, 5.2] | 2.3 [2.0, 2.9] |
| ln(CEA + 1) | 0.8 [0.6,1.2] | 1.1 [0.6, 1.5] | 1.1 [1.0, 1.2] | 1.4 [1.0, 2.0] | 1.1 [0.7, 1.4] | 1.1 [0.8, 1.5] | 0.9 [0.6, 1.7] | 1.6 [1.6, 1.6] | 0.9 [0.9, 1.3] | 1.0 [0.7, 1.6] |

[1]Median [Q1, Q3] for continuous variables; n (%) for categorical variables

[a] Not mutually exclusive; patients could have lesions in more than one location. SCN, serous cystadenoma; MCN, mucinous cystic neoplasm; IPMN, intraductal papillary mucinous neoplasm; SPN, solid pseudopapillary neoplasm; NET, neuroendocrine tumor; MPD, Main pancreatic duct; CBD, Common bile duct.

Note: Serum CA 19-9 and CEA concentrations were originally measured in U/mL and ng/mL, respectively. When log-transformed values are reported, the transformation is expressed as ln(CA 19-9 + 1) and ln(CEA + 1), respectively.

Table S8 Baseline Characteristics of the Prospective Cohort by Pathologic Diagnosis.

| Variable | Overall | SCN | IPMN | MCN | NET | SPN | Benign | Malignant | No pathology |
|---|---|---|---|---|---|---|---|---|---|
| N | 76 | 20 | 19 | 7 | 7 | 5 | 1 | 1 | 16 |

| Variable | Overall | SCN | IPMN | MCN | NET | SPN | Benign | Malignant | No pathology |
|---|---|---|---|---|---|---|---|---|---|
| Age (years) | 60 [52, 66] | 59 [51, 64] | 66 [62, 68] | 51 [44, 54] | 56 [54, 60] | 43 [40, 50] | 56 [56, 56] | 59 [59, 59] | 64 [60, 68] |
| Gender | | | | | | | | | |
| Female | 49 (64) | 15 (75) | 11 (58) | 7 (100) | 3 (43) | 3 (60) | 1 (100) | 0 (0) | 9 (56) |
| Male | 27 (36) | 5 (25) | 8 (42) | 0 (0) | 4 (57) | 2 (40) | 0 (0) | 1 (100) | 7 (44) |
| Long diameter of lesion (mm) | 32 [24, 46] | 36 [25, 43] | 32 [24, 44] | 51 [46, 76] | 25 [23, 36] | 44 [22, 66] | 42 [42, 42] | 32 [32, 32] | 26 [21, 32] |
| Short diameter of lesion(mm) | 23 [18, 35] | 27 [19, 35] | 22 [16, 26] | 38 [34, 61] | 23 [20, 34] | 35 [21, 51] | 21 [21, 21] | 25 [25, 25] | 20 [17, 26] |
| Long diameter of solid component (mm) | 0 [0, 0] | 0 [0, 0] | 0 [0, 0] | 0 [0, 0] | 22 [16, 31] | 28 [12, 38] | 0 [0, 0] | 14 [14, 14] | 0 [0, 0] |
| Short diameter of solid component (mm) | 0 [0, 0] | 0 [0, 0] | 0 [0, 0] | 0 [0, 0] | 14 [12, 19] | 21 [11, 30] | 0 [0, 0] | 10 [10, 10] | 0 [0, 0] |
| CA, 199 (U/mL) | 10 [7, 17] | 10 [7, 14] | 14 [8, 30] | 9 [7, 68] | 9 [9, 12] | 9 [7, 10] | 11 [11, 11] | 609 [609, 609] | 10 [0, 15] |
| CEA (ng/mL) | 2 [1, 2] | 1 [1, 2] | 2 [1, 2] | 1 [1, 1] | 1 [1, 2] | 2 [2, 2] | 2 [2, 2] | 2 [2, 2] | 2 [0, 2] |
| Jaundice | | | | | | | | | |
| Yes | 0 (0) | 0 (0) | 0 (0) | 0 (0) | 0 (0) | 0 (0) | 0 (0) | 0 (0) | 0 (0) |
| No | 76 (100) | 20 (100) | 19 (100) | 7 (100) | 7 (100) | 5 (100) | 1 (100) | 1 (100) | 16 (100) |
| Diabetes | | | | | | | | | |
| Yes | 13 (17) | 4 (20) | 2 (11) | 0 (0) | 3 (43) | 2 (40) | 0 (0) | 1 (100) | 1 (6) |
| No | 63 (83) | 16 (80) | 17 (89) | 7 (100) | 4 (57) | 3 (60) | 1 (100) | 0 (0) | 15 (94) |
| Cyst Lesion Type | | | | | | | | | |
| Cystic, solid | 17 (22) | 0 (0) | 1 (5) | 0 (0) | 7 (100) | 5 (100) | 0 (0) | 1 (100) | 3 (19) |
| Macrocystic | 30 (39) | 6 (30) | 11 (58) | 6 (86) | 0 (0) | 0 (0) | 0 (0) | 0 (0) | 7 (44) |
| Microcystic | 14 (18) | 11 (55) | 3 (16) | 0 (0) | 0 (0) | 0 (0) | 0 (0) | 0 (0) | 0 (0) |
| Unilocular | 15 (20) | 3 (15) | 4 (21) | 1 (14) | 0 (0) | 0 (0) | 1 (100) | 0 (0) | 6 (38) |
| Solid Component Enhancement | | | | | | | | | |
| Absent solid component | 55 (72) | 19 (95) | 17 (89) | 7 (100) | 0 (0) | 0 (0) | 1 (100) | 0 (0) | 11 (69) |
| Delayed enhancement | 15 (20) | 1 (5) | 1 (5) | 0 (0) | 4 (57) | 5 (100) | 0 (0) | 1 (100) | 3 (19) |
| Early arterial enhancement | 4 (5) | 0 (0) | 0 (0) | 0 (0) | 3 (43) | 0 (0) | 0 (0) | 0 (0) | 1 (6) |
| No enhancement | 2 (3) | 0 (0) | 1 (5) | 0 (0) | 0 (0) | 0 (0) | 0 (0) | 0 (0) | 1 (6) |
| Cyst Wall Thickness | | | | | | | | | |
| Absent cyst wall | 22 (29) | 2 (10) | 2 (11) | 0 (0) | 7 (100) | 5 (100) | 0 (0) | 1 (100) | 5 (31) |

| Variable | Overall | SCN | IPMN | MCN | NET | SPN | Benign | Malignant | No pathology |
|---|---|---|---|---|---|---|---|---|---|
| Thick, walled | 3 (4) | 0 (0) | 3 (16) | 0 (0) | 0 (0) | 0 (0) | 0 (0) | 0 (0) | 0 (0) |
| Thin, walled | 51 (67) | 18 (90) | 14 (74) | 7 (100) | 0 (0) | 0 (0) | 1 (100) | 0 (0) | 11 (69) |
| Cyst Wall Uniform | | | | | | | | | |
| Absent cyst wall | 22 (29) | 2 (10) | 2 (11) | 0 (0) | 7 (100) | 5 (100) | 0 (0) | 1 (100) | 5 (31) |
| Yes | 51 (67) | 17 (85) | 16 (84) | 6 (86) | 0 (0) | 0 (0) | 1 (100) | 0 (0) | 11 (69) |
| No | 3 (4) | 1 (5) | 1 (5) | 1 (14) | 0 (0) | 0 (0) | 0 (0) | 0 (0) | 0 (0) |
| Cyst Wall Enhancement | | | | | | | | | |
| Absent cyst wall | 22 (29) | 2 (10) | 2 (11) | 0 (0) | 7 (100) | 5 (100) | 0 (0) | 1 (100) | 5 (31) |
| Delayed enhancement | 17 (22) | 2 (10) | 8 (42) | 2 (29) | 0 (0) | 0 (0) | 0 (0) | 0 (0) | 5 (31) |
| No enhancement | 37 (49) | 16 (80) | 9 (47) | 5 (71) | 0 (0) | 0 (0) | 1 (100) | 0 (0) | 6 (38) |
| Intracystic Septations | | | | | | | | | |
| Absent septations | 39 (51) | 5 (25) | 7 (37) | 2 (29) | 7 (100) | 5 (100) | 1 (100) | 1 (100) | 11 (69) |
| Thick septations | 9 (12) | 2 (10) | 3 (16) | 0 (0) | 0 (0) | 0 (0) | 0 (0) | 0 (0) | 4 (25) |
| Thin septations | 28 (37) | 13 (65) | 9 (47) | 5 (71) | 0 (0) | 0 (0) | 0 (0) | 0 (0) | 1 (6) |
| Septations Uniform | | | | | | | | | |
| Absent septations | 39 (51) | 5 (25) | 7 (37) | 2 (29) | 7 (100) | 5 (100) | 1 (100) | 1 (100) | 11 (69) |
| Yes | 31 (41) | 14 (70) | 10 (53) | 5 (71) | 0 (0) | 0 (0) | 0 (0) | 0 (0) | 2 (12) |
| No | 6 (8) | 1 (5) | 2 (11) | 0 (0) | 0 (0) | 0 (0) | 0 (0) | 0 (0) | 3 (19) |
| Septations Enhancement | | | | | | | | | |
| Absent septations | 39 (51) | 5 (25) | 7 (37) | 2 (29) | 7 (100) | 5 (100) | 1 (100) | 1 (100) | 11 (69) |
| Delayed enhancement | 36 (47) | 14 (70) | 12 (63) | 5 (71) | 0 (0) | 0 (0) | 0 (0) | 0 (0) | 5 (31) |
| No enhancement | 1 (1) | 1 (5) | 0 (0) | 0 (0) | 0 (0) | 0 (0) | 0 (0) | 0 (0) | 0 (0) |
| PD Communication | | | | | | | | | |
| Yes | 32 (42) | 4 (20) | 19 (100) | 0 (0) | 0 (0) | 0 (0) | 1 (100) | 0 (0) | 8 (50) |
| No | 44 (58) | 16 (80) | 0 (0) | 7 (100) | 7 (100) | 5 (100) | 0 (0) | 1 (100) | 8 (50) |
| MPD Dilation | | | | | | | | | |
| Yes | 32 (42) | 4 (20) | 16 (84) | 0 (0) | 1 (14) | 0 (0) | 1 (100) | 0 (0) | 10 (62) |
| No | 44 (58) | 16 (80) | 3 (16) | 7 (100) | 6 (86) | 5 (100) | 0 (0) | 1 (100) | 6 (38) |
| MPD Diameter (mm) | 0 [0, 6] | 0 [0, 0] | 8 [4, 10] | 0 [0, 0] | 0 [0, 0] | 0 [0, 0] | 11 [11, 11] | 0 [0, 0] | 4 [2, 6] |
| Long diameter of largest mural nodule (mm) | 0 [0, 0] | 0 [0, 0] | 0 [0, 0] | 0 [0, 0] | 0 [0, 0] | 0 [0, 0] | 0 [0, 0] | 0 [0, 0] | 0 [0, 0] |

| Variable | Overall | SCN | IPMN | MCN | NET | SPN | Benign | Malignant | No pathology |
|---|---|---|---|---|---|---|---|---|---|
| Short diameter of largest mural nodule (mm) | 0 [0, 0] | 0 [0, 0] | 0 [0, 0] | 0 [0, 0] | 0 [0, 0] | 0 [0, 0] | 0 [0, 0] | 0 [0, 0] | 0 [0, 0] |
| Mural Nodule Enhancement | | | | | | | | | |
| Delayed enhancement | 1 (1) | 0 (0) | 0 (0) | 1 (14) | 0 (0) | 0 (0) | 0 (0) | 0 (0) | 0 (0) |
| No mural nodule | 75 (99) | 20 (100) | 19 (100) | 6 (86) | 7 (100) | 5 (100) | 1 (100) | 1 (100) | 16 (100) |
| Common Bile Duct (CBD) (mm) | 0 [0, 0] | 0 [0, 0] | 0 [0, 0] | 0 [0, 0] | 0 [0, 0] | 0 [0, 0] | 0 [0, 0] | 0 [0, 0] | 0 [0, 2] |
| Short diameter of largest lymph node (mm) | 0 [0, 0] | 0 [0, 0] | 0 [0, 0] | 0 [0, 0] | 0 [0, 0] | 0 [0, 0] | 0 [0, 0] | 0 [0, 0] | 0 [0, 0] |
| Capsule | | | | | | | | | |
| Yes | 6 (8) | 2 (10) | 0 (0) | 0 (0) | 0 (0) | 3 (60) | 0 (0) | 1 (100) | 0 (0) |
| No | 70 (92) | 18 (90) | 19 (100) | 7 (100) | 7 (100) | 2 (40) | 1 (100) | 0 (0) | 16 (100) |
| Lesion location | | | | | | | | | |
| Head and neck | 41 (54) | 8 (40) | 15 (79) | 1 (14) | 1 (14) | 4 (80) | 1 (100) | 1 (100) | 10 (62) |
| Body and tail | 35 (46) | 12 (60) | 4 (21) | 6 (86) | 6 (86) | 1 (20) | 0 (0) | 0 (0) | 6 (38) |

[1]Median [Q1, Q3] for continuous variables; n (%) for categorical variables

[a] Not mutually exclusive; patients could have lesions in more than one location. SCN, serous cystadenoma; MCN, mucinous cystic neoplasm; IPMN, intraductal papillary mucinous neoplasm; SPN, solid pseudopapillary neoplasm; NET, neuroendocrine tumor; MPD, Main pancreatic duct; CBD, Common bile duct.

Note: Serum CA 19-9 and CEA concentrations were originally measured in U/mL and ng/mL, respectively. When log-transformed values are reported, the transformation is expressed as ln(CA 19-9 + 1) and ln(CEA + 1), respectively.

## Appendix 4. Pathological classification model development and temporal validation

*4.1 Model overview*

These formulas calculate the linear Score for each class. In a multi-class logistic regression model, the probability for a specific class $k$ is typically calculated using the Softmax function:

$$P(Y=k)=\frac{e^{Score_k}}{\sum_j e^{Score_j}}$$

where k represents the specific risk group (IPMN, MCN, SCN, NET, or SPN).

*4.2 Standardization parameters*

During the model development, continuous variables were standardized to ensure convergence and comparability. The formula for standardization was $Z=(X-\square)/\square$, where X is the raw value, $\square$ is the mean, and $\square$ is the standard deviation, calculated with the full datasets of IPMN.

Based on the coefficients and standardization parameters provided, the continuous variables (Age, CA 19-9, CEA, and Long diameter of lesion) have been unstandardized. The adjusted intercept and coefficients are presented below in Table S8.

Table S9. Parameters for variable standardization in five-class stratification model

| Feature | Mean ($\square$) | Standard Deviation ($\square$) |
|---|---|---|
| Age (years) | 53.42 | 13.84 |
| ln(CA 19-9 + 1) | 2.94 | 1.47 |
| ln(CEA + 1) | 1.15 | 0.59 |
| Long diameter of lesion (mm) | 44.35 | 24.08 |

Note: CA 19-9 and CEA values were log-transformed prior to standardization and model fitting to address skewness in their distributions. CA19-9=ln(CA19-9+1); CEA =ln(CEA+1)

*4.3 Prediction score formulas for pathological classification prediction*

The following formulas calculate the linear predictive score for each risk group.

**Score (IPMN)** = 0.5486 + 1.1625 × Z(Age) + 0.4693 × Z(Ln_CA199) + 0.0415 × Z(Ln_CEA) - 0.1520 × Capsule - 0.7199 × Cyst wall enhancement (Delayed enhancement) + 0.4801 × Cyst wall enhancement (No enhancement) - 0.4607 × Cyst wall thickness (Absent cyst wall) + 0.3446 × Cyst wall thickness (Thin-walled) - 0.7018 × Gender + 0.5112 × Intracystic septations (Thin septations) + 0.0893 × Lesion (Head/neck) - 0.3223 × Z(Lesion_Size) - 0.0636 × MPD dilation + 2.7700 × PD communication - 0.1362 × Pancreatic parenchymal atrophy - 0.5384 × Solid component enhancement (Arterial Phase) - 0.1446 × Solid component enhancement (Delayed enhancement) - 0.0280 × Tumor lesion (Macrocystic) - 0.6267 × Tumor lesion (Microcystic) + 0.0178 × Uniform Cyst wall (Yes) + 0.1332 × Vascular abutment

**Score (MCN)** = 0.0509 + 0.3128 × Z(Age) + 0.3520 × Z(Ln_CA199) + 0.0420 × Z(Ln_CEA) - 0.5297 × Capsule + 0.5171 × Cyst wall enhancement (Delayed enhancement) + 0.8061 × Cyst wall enhancement (No enhancement) - 0.3749 × Cyst wall thickness (Absent cyst wall) + 0.4877 × Cyst wall thickness (Thin-walled) + 0.3236 × Gender + 0.2705 × Intracystic septations (Thin septations) - 0.3335 × Lesion (Head/neck) + 0.1432 × Z(Lesion_Size) + 0.4306 × MPD dilation + 0.0778 × PD communication + 0.1719 × Pancreatic parenchymal atrophy - 1.0540 × Solid component enhancement (Arterial Phase) - 0.0074 × Solid component enhancement

(Delayed enhancement) + 0.2197 × Tumor lesion (Macrocystic) - 0.8729 × Tumor lesion (Microcystic) + 0.4119 × Uniform Cyst wall (Yes) + 0.2778 × Vascular abutment

**Score (SCN)** = -0.1390 + 0.3133 × Z(Age) - 0.1666 × Z(Ln_CA199) - 0.0398 × Z(Ln_CEA) - 1.0142 × Capsule - 0.1818 × Cyst wall enhancement (Delayed enhancement) - 0.3776 × Cyst wall enhancement (No enhancement) + 0.1829 × Cyst wall thickness (Absent cyst wall) + 1.3603 × Cyst wall thickness (Thin-walled) + 0.4457 × Gender + 0.4544 × Intracystic septations (Thin septations) - 0.0476 × Lesion (Head/neck) + 0.0417 × Z(Lesion_Size) - 0.2049 × MPD dilation - 0.7160 × PD communication + 0.5271 × Pancreatic parenchymal atrophy + 0.2503 × Solid component enhancement (Arterial Phase) - 0.2560 × Solid component enhancement (Delayed enhancement) + 0.0004 × Tumor lesion (Macrocystic) + 1.4820 × Tumor lesion (Microcystic) + 0.3961 × Uniform Cyst wall (Yes) + 0.1692 × Vascular abutment

**Score (SPN)** = -1.4357 - 1.7639 × Z(Age) - 0.4690 × Z(Ln_CA199) - 0.2407 × Z(Ln_CEA) + 1.4632 × Capsule + 0.3207 × Cyst wall enhancement (Delayed enhancement) - 0.3269 × Cyst wall enhancement (No enhancement) + 0.3533 × Cyst wall thickness (Absent cyst wall) - 1.0665 × Cyst wall thickness (Thin-walled) + 0.1526 × Gender - 0.2797 × Intracystic septations (Thin septations) + 0.1260 × Lesion (Head/neck) + 0.0727 × Z(Lesion_Size) - 0.1666 × MPD dilation - 0.8299 × PD communication - 0.2738 × Pancreatic parenchymal atrophy - 0.3767 × Solid

component enhancement (Arterial Phase) + 0.6459 × Solid component enhancement (Delayed enhancement) - 0.0562 × Tumor lesion (Macrocystic) - 0.1537 × Tumor lesion (Microcystic) - 0.4971 × Uniform Cyst wall (Yes) - 0.2475 × Vascular abutment

**Score (NET)** = 0.9752 - 0.0248 × Z(Age) - 0.1858 × Z(Ln_CA199) + 0.1969 × Z(Ln_CEA) + 0.2328 × Capsule + 0.0639 × Cyst wall enhancement (Delayed enhancement) - 0.5818 × Cyst wall enhancement (No enhancement) + 0.2993 × Cyst wall thickness (Absent cyst wall) - 1.1262 × Cyst wall thickness (Thin-walled) - 0.2201 × Gender - 0.9563 × Intracystic septations (Thin septations) + 0.1657 × Lesion (Head/neck) + 0.0647 × Z(Lesion_Size) + 0.0045 × MPD dilation - 1.3020 × PD communication - 0.2890 × Pancreatic parenchymal atrophy + 1.7188 × Solid component enhancement (Arterial Phase) - 0.2379 × Solid component enhancement (Delayed enhancement) - 0.1358 × Tumor lesion (Macrocystic) + 0.1714 × Tumor lesion (Microcystic) - 0.3287 × Uniform Cyst wall (Yes) - 0.3328 × Vascular abutment

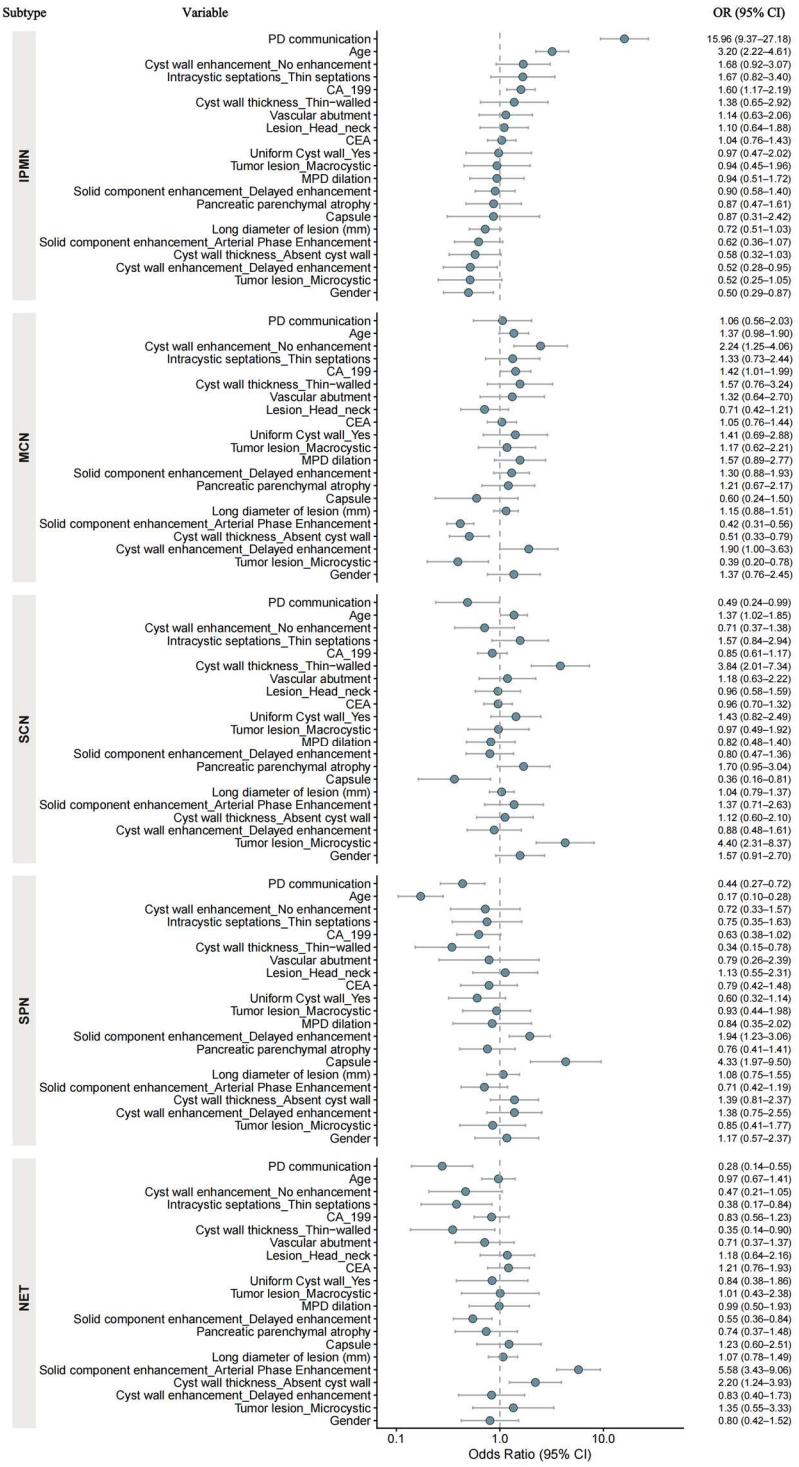


Figure S11. Odds ratios and 95% confidence intervals for clinical and imaging features associated with five-category pathological classification of PCLs using multinomial logistic regression.

*4.4 SHAP analysis and DCA analysis for the five category model*

Stacked bar chart displaying the mean absolute SHAP (SHapley Additive exPlanations) values for each feature across five pancreatic cystic neoplasm subtypes: serous cystic neoplasm (SCN), intraductal papillary mucinous neoplasm (IPMN), mucinous cystic neoplasm (MCN), solid pseudopapillary neoplasm (SPN), and pancreatic neuroendocrine tumour (NET). Features are ranked in descending order of overall importance. Main pancreatic duct (PD) communication demonstrated the highest predictive value, followed by tumour lesion morphology (microcystic pattern) and patient age. The length of each coloured segment represents the contribution of that feature to distinguishing each tumour subtype. SHAP values were calculated directly from the final multinomial logistic regression model using a model-agnostic explanation approach to quantify the contribution of individual predictors to model predictions of five-category classification (Figure S1).

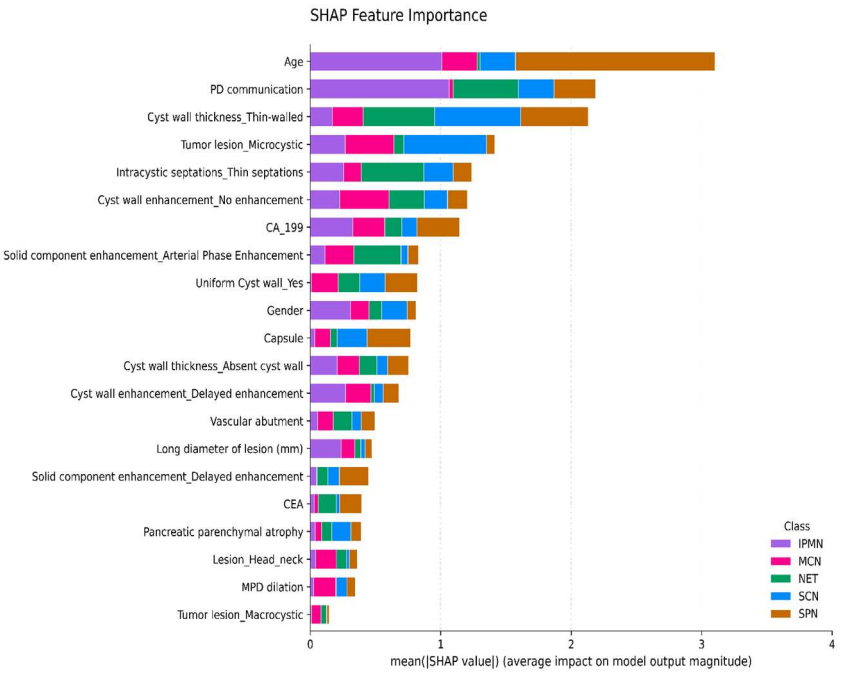

Figure S12. Mean absolute SHAP values showing the relative importance of clinical and imaging features in predicting pancreatic cystic neoplasm subtypes in five-class classification model.

Table S10. Cross-tabulation analysis of the five-category pathological classification model in three cohorts

| Cohort | | Truth / Prediction | Histologic Types, n (column %) | | | | |
|---|---|---|---|---|---|---|---|
| | | | IPMN | MCN | NET | SCN | SPN |
| Training cohort | Model | IPMN | 133(80.6) | 19(17.9) | 4 (6.0) | 17 (8.6) | 0 (0.0) |
| | | MCN | 14 (8.5) | 51(48.1) | 2 (3.0) | 27 (13.7) | 1 (1.5) |
| | | NET | 2 (1.2) | 2 (1.9) | 52(77.6) | 9 (4.6) | 5 (7.7) |
| | | SCN | 16 (9.7) | 33(31.1) | 5 (7.5) | 143(72.6) | 4 (6.2) |
| | | SPN | 0 (0.0) | 1 (0.9) | 4 (6.0) | 1 (0.5) | 55(84.6) |
| Internal validation cohort | Model | IPMN | 56 (78.9) | 8 (17.4) | 1 (3.4) | 6 (7.1) | 0 (0.0) |
| | | MCN | 6 (8.5) | 28(60.9) | 1 (3.4) | 10 (11.9) | 1 (3.6) |
| | | NET | 0 (0.0) | 1 (2.2) | 22(75.9) | 3 (3.6) | 1 (3.6) |
| | | SCN | 9 (12.7) | 9 (19.6) | 3 (10.3) | 63 (75.0) | 3 (10.7) |
| | | SPN | 0 (0.0) | 0 (0.0) | 2 (6.9) | 2 (2.4) | 23(82.1) |
| Temporal validation cohort | Model | IPMN | 70 (89.7) | 4 (12.1) | 1 (5.6) | 12 (16.2) | 0 (0.0) |
| | | MCN | 5 (6.4) | 18(54.5) | 1 (5.6) | 12 (16.2) | 3 (7.3) |
| | | NET | 2 (2.6) | 0 (0.0) | 9 (50.0) | 4 (5.4) | 8 (19.5) |
| | | SCN | 1 (1.3) | 9 (27.3) | 5 (27.8) | 46 (62.2) | 0 (0.0) |
| | | SPN | 0 (0.0) | 2 (6.1) | 2 (11.1) | 0 (0.0) | 30(73.2) |

Indeterminate indicates that the radiologist did not assign a specific subtype among IPMN, MCN, NET, SCN, and SPN. Abbreviations: IPMN, intraductal papillary mucinous neoplasm; MCN, mucinous cystic neoplasm; NET, neuroendocrine tumor; SCN, serous cystadenoma; SPN, solid pseudopapillary

**Evaluation of diagnostic accuracy and clinical decision outcomes**

The diagnostic performance of SIRS-PCL was compared with that of radiologists using the Hong Kong consensus guidelines in the complete-case temporal validation cohort (n = 211), with postoperative histopathological findings serving as the reference standard.

Five-category pathological classification accuracy was calculated as the proportion of patients whose predicted pathological subtype exactly matched the final

histopathological diagnosis. For the end-to-end assessment of real-world clinical practice, a prediction was considered correct if the pathological subtype was accurately identified or if a pathologically confirmed low-risk IPMN/MCN or SCN was classified as benign, reflecting clinically equivalent management decisions. The overall end-to-end accuracy was calculated as the proportion of correctly classified patients among all 211 patients.

Clinical decision outcomes were evaluated using pathology-defined reference groups. Unnecessary surgery and over-examination were assessed among patients with pathologically confirmed low-risk IPMN/MCN or SCN, whereas missed diagnosis was evaluated among patients with pathologically confirmed high-risk IPMN/MCN, SPN, or NET. Unnecessary surgery was defined as the classification of a low-risk lesion into a category warranting surgical intervention, while over-examination was defined as its classification into a category requiring additional diagnostic evaluation. Missed diagnosis was defined as the classification of a high-risk lesion into a benign or low-risk management category.

The same pathological reference groups and clinical decision criteria were applied to SIRS-PCL and radiologist assessment combined with the Hong Kong consensus guidelines to ensure comparability. Overall accuracy was reported with 95% confidence intervals calculated using the Wilson score method. The results of decsion curve analysis are presented in **Figure S13.**

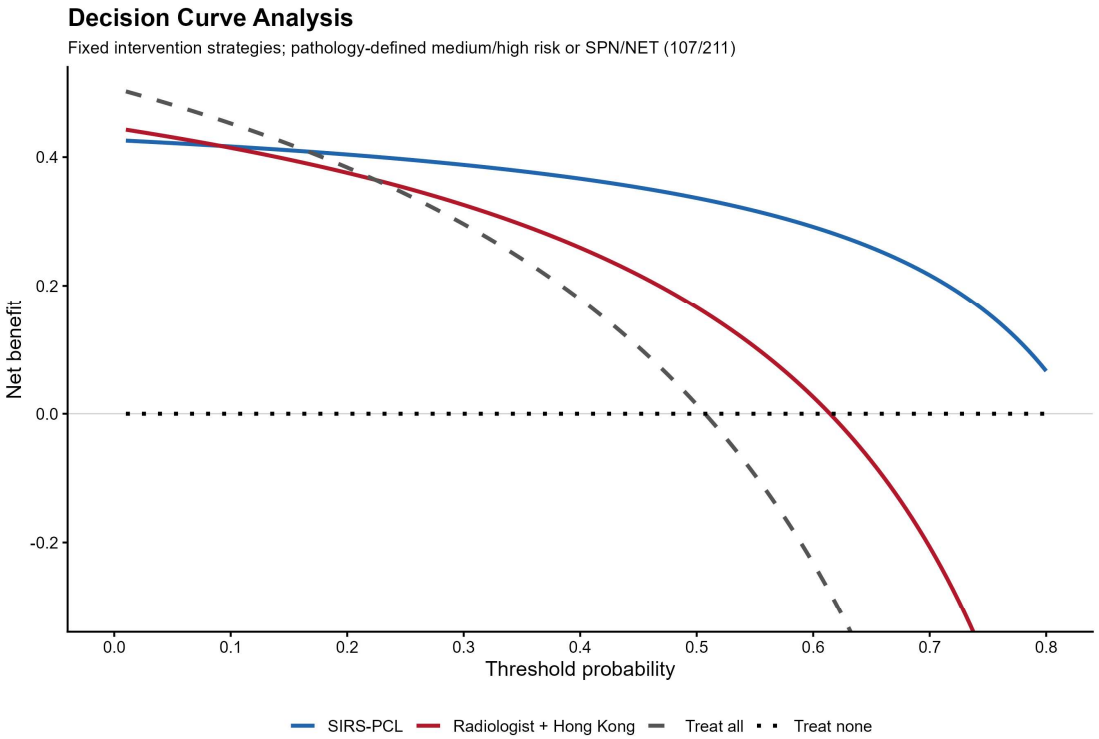


Figure S13. Decision Curve Analysis results of SIRS-PCL versus real-world clinical practice for end-to-end assessment. Pathological classification & risk stratification confusion matrix diagram using an temporal validation cohort with complete data.

Abbreviations: ACG: the American College of Gastroenterology; ESG: endoscopic ultrasound; HK: Hong Kong; SIRS-PCL: the Pancreatic Cystic Lesions Structured Imaging Reports System.

Table S11. Net benefit of SIRS-PCL and radiologist assessment plus Hong Kong consensus across representative threshold probabilities

| Threshold probability | SIRS-PCL | Radiologist + Hong Kong | Treat all | Treat none | Difference in net benefit* |
|---|---|---|---|---|---|
| 0.05 | 0.422 | 0.431 | 0.481 | 0.000 | − 0.009 |
| 0.10 | 0.417 | 0.414 | 0.452 | 0.000 | 0.002 |
| 0.20 | 0.404 | 0.376 | 0.384 | 0.000 | 0.028 |
| 0.30 | 0.388 | 0.326 | 0.296 | 0.000 | 0.062 |
| 0.40 | 0.367 | 0.259 | 0.179 | 0.000 | 0.107 |
| 0.50 | 0.337 | 0.166 | 0.014 | 0.000 | 0.171 |
| 0.60 | 0.292 | 0.026 | − 0.2322 | 0.000 | 0.265 |

[a].Difference in net benefit = SIRS-PCL − radiologist assessment plus Hong Kong consensus.

Decision curve analysis was performed to compare the net benefit of SIRS-PCL with real-world clinical practice (radiologist assessment combined with the Hong Kong consensus guidelines). Figure S12 and Table S11 show that the two strategies

yielded comparable net benefits at lower threshold probabilities (0.05 – 0.10). At threshold probabilities of 0.10 – 0.60, SIRS-PCL demonstrated consistently greater net benefit than radiologist assessment combined with guideline-based interpretation, with the difference becoming more pronounced at higher thresholds.

We performed subgroup analyses according to imaging modality to assess the diagnostic performance of SIRS-PCL in CT- and MRI-based examinations for five category prediction in Table S12.

Table S12. Comparison of the diagnostic performance of CT- and MRI-based examinations for five-category prediction in the complete cases of the temporal validation cohort

| Imaging | Class | Sensitivity | Specificity | AUC |
|---|---|---|---|---|
| CT (n=140) | IPMN | 0.89 (0.80-0.97) | 0.92 (0.87-0.98) | 0.96 (0.91-0.99) |
| | MCN | 0.59 (0.38-0.81) | 0.92 (0.87-0.96) | 0.93 (0.89-0.97) |
| | PNEP | 0.46 (0.17-0.80) | 0.95 (0.90-0.98) | 0.89 (0.79-0.97) |
| | SCN | 0.64 (0.50-0.79) | 0.88 (0.82-0.95) | 0.89 (0.83-0.94) |
| | SPN | 0.86 (0.69-1.00) | 0.99 (0.97-1.00) | 0.98 (0.95-1.00) |
| MRI (n=71) | IPMN | 0.91 (0.78-1.00) | 0.92 (0.83-0.98) | 0.97 (0.93-1.00) |
| | MCN | 0.23 (0.00-1.00) | 0.89 (0.82-0.97) | 0.83 (0.67-0.96) |
| | PNEP | 0.58 (0.20-1.00) | 0.91 (0.82-0.97) | 0.86 (0.66-0.99) |
| | SCN | 0.65 (0.43-0.84) | 0.96 (0.91-1.00) | 0.95 (0.90-0.99) |
| | SPN | 0.65 (0.41-0.88) | 0.96 (0.90-1.00) | 0.96 (0.90-1.00) |

## Appendix 5. IPMN risk stratification model development and temporal validation

*5.1 Model overview*

This prediction model was developed to categorize patients with IPMN into three risk groups based on clinical and imaging features: Low Risk, Medium Risk, and High Risk. The model utilizes a multi-class logistic regression algorithm. For each patient, a linear Score is calculated for each of the three risk groups. These scores are then converted into probabilities using the Softmax function:

$$P(k)=\frac{e^{Score_k}}{\sum_j e^{Score_j}}$$

where k represents the specific risk group (Benign/Low Risk, Medium Risk, or High Risk).

*5.2 Standardization parameters*

During the model development, continuous variables were standardized to ensure convergence and comparability. The formula for standardization was $Z=(X-\square)/\square$, where X is the raw value, $\square$ is the mean, and $\square$ is the standard deviation, calculated with the full datasets of IPMN.

To facilitate clinical application, the prediction formulas provided in Section 3 have been mathematically adjusted (un-standardized). This allows users to input raw clinical values directly without manual standardization. The statistical parameters used for this adjustment are listed in Table S13.

Table S13. Parameters for Variable Standardization

| Feature | Mean (□) | Standard Deviation (□) |
|---|---|---|
| Age (years) | 61.63 | 8.25 |
| ln(CA 19-9 + 1) | 3.59 | 1.76 |
| ln(CEA + 1) | 1.42 | 0.62 |
| Diameter of MPD (mm) | 7.51 | 5.57 |
| Long diameter of largest mural nodule (mm) | 1.11 | 4.13 |
| Long diameter of lesion (mm) | 37.82 | 17.73 |
| Long diameter of solid component (mm) | 12.06 | 18.93 |
| Short diameter of largest lymph node (mm) | 0.63 | 2.70 |
| Short diameter of largest mural nodule (mm) | 0.91 | 3.53 |
| Short diameter of lesion (mm) | 27.32 | 13.85 |
| Short diameter of solid component (mm) | 9.26 | 14.74 |

Note: CA 19-9 and CEA values were log-transformed prior to standardization and model fitting to address skewness in their distributions. CA19-9=ln(CA19-9+1); CEA =ln(CEA+1)

*5.3 Prediction score formulas for IPMN risk prediction*

The following formulas calculate the linear predictive score for each risk group, using the standardized coefficients derived from the pooled analysis. Categorical variables are coded as 1 (Present) or 0 (Absent).

**Score (Low Risk)**= -0.8666 - 0.4327 × $Z_{Ln(CA19\text{-}9)}$ - 0.0171 × $Z_{Ln(CEA)}$ + 0.1985 × Cyst wall enhancement (Enhancement) - 0.2015 × Cyst wall enhancement (No enhancement) + 0.0005 × Cyst wall thickness (Absent cyst wall) - 0.5194 × Cyst wall thickness (Thick-walled) + 0.5163 × Cyst wall thickness (Thin-walled) - 0.4055 × $Z_{Diameter\ of\ MPD}$ - 0.5634 × $Z_{Long\ diameter\ of\ lesion}$ - 0.6004 × Uniform Cyst wall (No) + 0.5974 × Uniform Cyst wall (Yes) + 0.2551 × Uniform Septations (Absent septations) - 0.5213 × Uniform Septations (No) + 0.2636 × Uniform Septations (Yes) - 0.6168 × Vascular abutment

**Score (Medium Risk)**= -0.1386 - 0.0686 × $Z_{Ln(CA19\text{-}9)}$ + 0.1825 × $Z_{Ln(CEA)}$ - 0.0383 × Cyst wall enhancement (Enhancement) + 0.3188 × Cyst wall enhancement (No enhancement) - 0.2766 × Cyst wall thickness (Absent cyst wall) + 0.3491 × Cyst wall thickness (Thick-walled) - 0.0685 × Cyst wall thickness (Thin-walled) + 0.1282 × $Z_{Diameter\ of\ MPD}$ + 0.0982 × $Z_{Long\ diameter\ of\ lesion}$ + 0.2843 × Uniform Cyst wall (No) - 0.0037 × Uniform Cyst wall (Yes) - 0.3670 × Uniform Septations (Absent septations) + 0.3018 × Uniform Septations (No) + 0.0691 × Uniform Septations (Yes) - 0.3215 × Vascular abutment

**Score (High Risk)** = 1.0052 + 0.5013 × $Z_{Ln(CA19\text{-}9)}$ - 0.1653 × $Z_{Ln(CEA)}$ - 0.1602 × Cyst wall enhancement (Enhancement) - 0.1173 × Cyst wall enhancement (No enhancement) + 0.2761 × Cyst wall thickness (Absent cyst wall) + 0.1703 × Cyst wall thickness (Thick-walled) - 0.4478 × Cyst wall thickness (Thin-walled) + 0.2773 × $Z_{Diameter\ of\ MPD}$ + 0.4652 × $Z_{Long\ diameter\ of\ lesion}$ + 0.3162 × Uniform Cyst wall (No) - 0.5936 × Uniform Cyst wall (Yes) + 0.1118 × Uniform Septations (Absent septations) + 0.2195 × Uniform Septations (No) - 0.3327 × Uniform Septations (Yes) + 0.9383 × Vascular abutment

*5.4 SHAP analysis and ROC curve for the IPMN risk stratification model*

Table S14. Comparison of the proposed IPMN risk stratification model and guideline-based classification in complete-data temporal validation (N=70).

| Model | Truth / Prediction | Pathology-confirmed IPMN (reference standard) N = 70 | | | |
|---|---|---|---|---|---|
| | | Low risk | Medium risk | High risk | Accuracy (%) |
| IPMN risk stratification model | Low risk | 18 (75.0) | 4 (50.0) | 4 (10.5) | 77.1 |
| | Medium risk | 3 (12.5) | 3 (37.5) | 1 (2.6) | |
| | High risk | 3 (12.5) | 1 (12.5) | 33 (86.8) | |
| Kyoto | Low risk | 3 (12.5) | 1 (12.5) | 1 (2.6) | 50.0 |
| | Medium risk | 15 (62.5) | 4 (50.0) | 9 (23.7) | |
| | High risk | 6 (25.0) | 3 (37.5) | 28 (73.7) | |
| ESG | Low risk | 16 (66.7) | 5 (62.5) | 11 (28.9) | 58.6 |
| | Medium risk | 2 (8.3) | 0 (0.0) | 2 (5.3) | |
| | High risk | 6 (25.0) | 3 (37.5) | 25 (65.8) | |
| Hong Kong | Low risk | 3 (12.5) | 1 (12.5) | 2 (5.3) | 51.4 |
| | Medium risk | 14 (58.3) | 4 (50.0) | 7 (18.4) | |
| | High risk | 7 (29.2) | 3 (37.5) | 29 (76.3) | |
| ACG* | Low risk | 3 (12.5) | 0 (0) | 1 (2.6) | 58.6 |
| | Medium risk | 0 (0.0) | 1(12.5) | 0 (0.0) | |
| | High risk | 21(87.5) | 7 (87.5) | 37 (97.4) | |

Indeterminate indicates that the radiologist did not assign a specific subtype among Low risk Medium risk. Abbreviations: IPMN, intraductal papillary mucinous neoplasm; MCN, mucinous cystic neoplasm; NET, neuroendocrine tumor; SCN, serous cystadenoma; SPN, solid pseudopapillary; ESG, the European Study Group on Cystic Tumors of the Pancreas; ACG, the American College of Gastroenterology.

*ACG: For the ACG guideline, patients meeting any ACG-defined concerning criteria were classified as high risk, whereas those without these features were classified as low risk. The ACG guideline does not define a separate intermediate-risk category. For performance evaluation, pathologically confirmed low- and intermediate-risk lesions were combined into the non-high-risk group, whereas high-risk lesions were evaluated separately.

Stacked bar chart displaying the mean absolute SHAP (SHapley Additive exPlanations) values for each feature across three IPMN risk categories: high risk (blue), low risk (pink), and medium risk (olive). Features are ranked in descending order of overall importance. Vascular abutment demonstrated the highest predictive value (mean |SHAP| ≈0.19), followed by long diameter of lesion and CA 19-9. The length of each coloured segment represents the contribution of that feature to

distinguishing each risk category. Notably, vascular abutment and lesion size contributed predominantly to high-risk classification, whilst uniform cyst wall and thin-walled cyst thickness were more important for low-risk classification. SHAP values were calculated directly from the final multinomial logistic regression model using a model-agnostic explanation approach to quantify the contribution of individual predictors to IPMN model predictions (Figure S13).

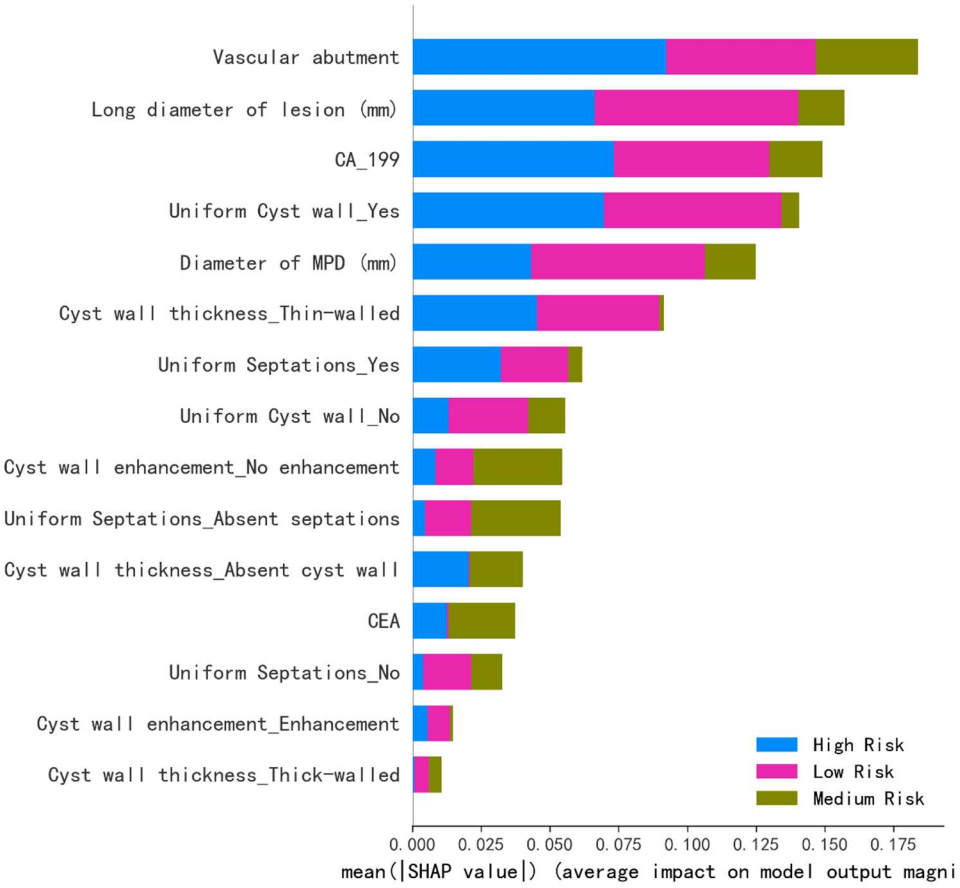


Figure S14. Mean absolute SHAP values showing the relative importance of clinical and imaging features in IPMN risk prediction.

Abbreviations: CA 19-9, carbohydrate antigen 19-9; CEA, carcinoembryonic antigen; CI, confidence interval; IPMN, intraductal papillary mucinous neoplasm; MPD, main pancreatic duct; OR, odds ratio; SHAP, SHapley Additive exPlanation

Forest plot presenting odds ratios (ORs) with 95 confidence intervals (CIs) for

15 clinical and imaging features across three IPMN risk categories: low risk, medium risk, and high risk (Figure S14). For low-risk IPMN, uniform cyst wall (OR 1.82, 95 CI 1.14–2.89) and thin-walled cyst (OR 1.68, 95 CI 0.98–2.86) were positively associated, whereas smaller lesion diameter (OR 0.57, 95 CI 0.38–0.86) was protective. For high-risk IPMN, vascular abutment showed the strongest association (OR 2.56, 95 CI 1.10–5.94), followed by larger lesion diameter (OR 1.59, 95 CI 1.06–2.40) and elevated CA 19-9 (OR 1.65, 95 CI 0.94–2.89).

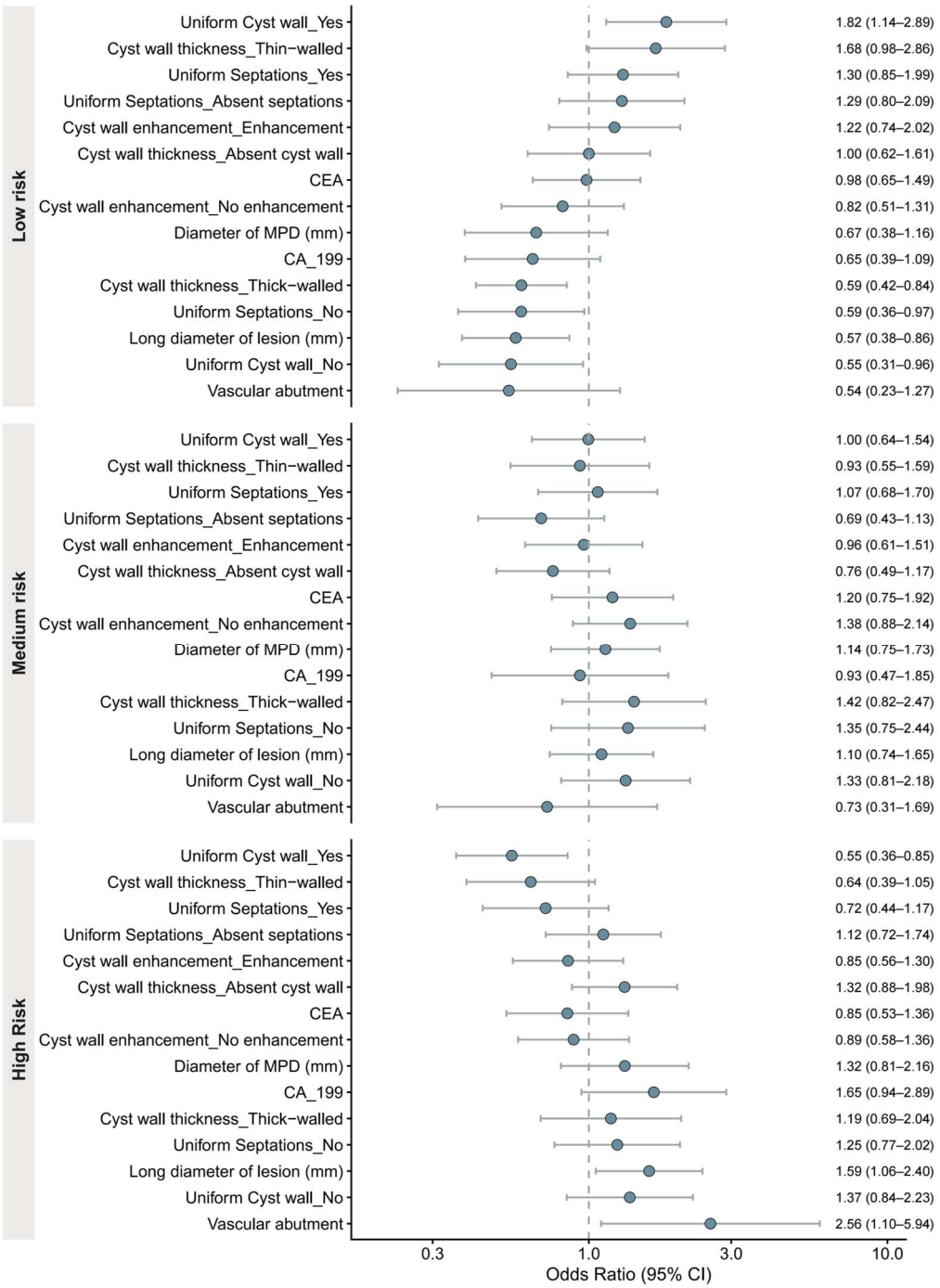


Figure S15. Odds ratios and 95 confidence intervals for clinical and radiological features associated with three risk categories of IPMN from multinomial logistic regression analysis.

Cross-tabulation of IPMN risk stratification model is presented in Table S14, and related ROC curve is demonstrated in Figure S16.

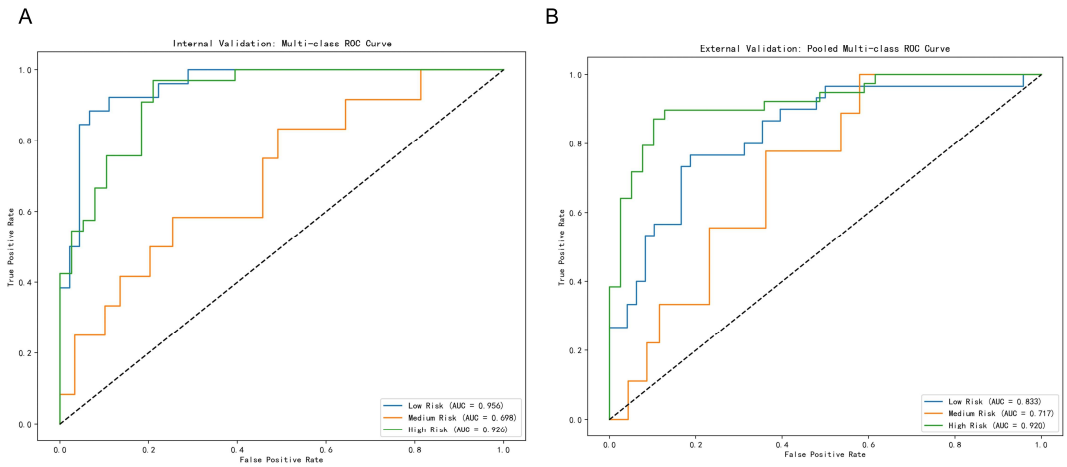


Figure S16. ROC curve of IPMN for internal and temporal validation. (A) ROC curve of IPMN for internal validation; (B) ROC curve of IPMN for temporal validation.

We performed subgroup analyses according to imaging modality to assess the diagnostic performance of SIRS-PCL in CT- and MRI-based examinations for IPMN risk prediction in Table S15.

Table S15. Comparison of the diagnostic performance of CT- and MRI-based examinations for IPMN pathological risk prediction in the complete cases of the temporal validation cohort

| Imaging | Class | Sensitivity | Specificity | AUC |
|---|---|---|---|---|
| CT (n = 47) | Low Risk | 0.69 (0.43-0.91) | 0.81 (0.66-0.94) | 0.79 (0.63-0.92) |
| | Medium Risk | 0.20 (0.00-0.67) | 0.95 (0.88-1.00) | 0.72 (0.50-0.90) |
| | High Risk | 0.89 (0.75-1.00) | 0.81 (0.63-0.96) | 0.89 (0.79-0.97) |
| MRI (n = 23) | Low Risk | 0.88 (0.60-1.00) | 0.86 (0.67-1.00) | 0.95 (0.83-1.00) |
| | Medium Risk | 0.67 (0.00-1.00) | 0.90 (0.75-1.00) | 0.75 (0.37-0.99) |
| | High Risk | 0.83 (0.58-1.00) | 1.00 (1.00-1.00) | 0.98 (0.91-1.00) |

## Appendix 6. MCN risk stratification model development and temporal validation

*6.1 Model overview*

This prediction model was developed to categorize patients with MCN into three risk groups based on clinical and imaging features: Benign/Low Risk, Medium Risk, and High Risk. The model utilizes a multi-class logistic regression algorithm. For each patient, a linear Score is calculated for each of the three risk groups. These scores are then converted into probabilities using the Softmax function:

$$P(k)=\frac{e^{Score_k}}{\sum_j e^{Score_j}}$$

where $k$ represents the specific risk group (Benign/Low Risk, Medium Risk, or High Risk).

*6.2 Standardization parameters*

During the model development, continuous variables were standardized to ensure convergence and comparability. The formula for standardization was $Z=(X-\mu)/\sigma$, where X is the raw value, $\mu$ is the mean, and $\sigma$ is the standard deviation, calculated with the full datasets of MCN (Table S16).

To facilitate clinical application, the prediction formulas provided in section 6.3 have been mathematically adjusted (un-standardized). This allows users to input raw clinical values directly without manual standardization.

Table S16 The statistical parameters used for this adjustment.

| Feature | Mean ($\mu$) | Standard Deviation ($\sigma$) |
|---|---|---|
| Age (years) | 52.13 | 13.71 |
| ln(CA 19-9 + 1) | 3.24 | 1.49 |
| ln(CEA + 1) | 1.15 | 0.71 |

| Feature | Mean (□) | Standard Deviation (□) |
|---|---|---|
| Diameter of MPD (mm) | 2.12 | 3.25 |
| Long diameter of largest mural nodule (mm) | 1.79 | 4.84 |
| Long diameter of lesion (mm) | 46.86 | 27.14 |
| Long diameter of solid component (mm) | 4.82 | 14.28 |
| Short diameter of largest lymph node (mm) | 0.12 | 1.22 |
| Short diameter of largest mural nodule (mm) | 1.42 | 3.99 |
| Short diameter of lesion (mm) | 38.31 | 21.88 |
| Short diameter of solid component (mm) | 3.68 | 10.66 |

Note: CA 19-9 and CEA values were log-transformed prior to standardization and model fitting to address skewness in their distributions.

*6.3 Prediction score formulas for MCN risk prediction*

The following formulas calculate the linear predictive score for each risk group.

**Score (Benign/Low Risk)** = 0.9268 - 0.1690 × Diabetes - 0.1508 × $Z_{Age}$ - 0.0376 × Cyst wall enhancement (Absent cyst wall) - 0.2860 × Cyst wall enhancement (Enhancement) + 0.3185 × Cyst wall enhancement (No enhancement) + 0.8186 × Lesion body tail - 0.7805 × Uniform Cyst wall (No) + 0.8130 × Uniform Cyst wall (Yes) + 0.0050 × $Z_{\text{Short diameter of largest mural nodule}}$ - 0.0334 × $Z_{\text{Short diameter of solid component}}$ - 0.0376 × Tumor lesion (Cystic-solid) - 0.4504 × Tumor lesion (Macrocystic) - 0.2167 × Tumor lesion (Microcystic) + 0.6996 × Tumor lesion (Unilocular) - 0.7047 × Vascular abutment

**Score (Medium Risk)** = -1.0611 - 0.3304 × Diabetes - 0.0045 × $Z_{Age}$ - 0.2375 × Cyst wall enhancement (Absent cyst wall) + 0.1940 × Cyst wall enhancement (Enhancement) + 0.0380 × Cyst wall enhancement (No enhancement) - 0.1506 × Lesion body tail + 0.3437 × Uniform Cyst wall (No) - 0.1117 × Uniform Cyst wall (Yes) - 0.6214 × $Z_{\text{Short diameter of largest mural nodule}}$ - 0.4737 ×

$Z_{\text{Short diameter of solid component}}$ - 0.2375 × Tumor lesion (Cystic-solid) + 0.3416 × Tumor lesion (Macrocystic) + 0.0121 × Tumor lesion (Microcystic) - 0.1217 × Tumor lesion (Unilocular) + 0.2682 × Vascular abutment

**Score (High Risk)** = 0.1343 + 0.4993 × Diabetes + 0.1553 × $Z_{\text{Age}}$ + 0.2751 × Cyst wall enhancement (Absent cyst wall) + 0.0920 × Cyst wall enhancement (Enhancement) - 0.3565 × Cyst wall enhancement (No enhancement) - 0.6680 × Lesion body tail + 0.4368 × Uniform Cyst wall (No) - 0.7013 × Uniform Cyst wall (Yes) + 0.6164 × $Z_{\text{Short diameter of largest mural nodule}}$ + 0.5071 × $Z_{\text{Short diameter of solid component}}$ + 0.2751 × Tumor lesion (Cystic-solid) + 0.1088 × Tumor lesion (Macrocystic) + 0.2047 × Tumor lesion (Microcystic) - 0.5780 × Tumor lesion (Unilocular) + 0.4365 × Vascular abutment

*6.4 SHAP analysis and ROC curve for the MCN risk stratification model*

Table S17. Cross-tabulation of MCN risk stratification model

| Cohort | Truth / Prediction | Pathological risk stratification, n (column ) | | |
|---|---|---|---|---|
| | | Benign/Low risk | Medium risk | High risk |
| Hongkong Guidelines | Benign/low risk | 5 | 0 | 0 |
| | Medium risk | 15 | 1 | 1 |
| | High risk | 1 | 0 | 3 |
| ACG Guidelines | Benign/low risk | 5 | 0 | 0 |
| | Medium risk | 0 | 0 | 0 |
| | High risk | 16 | 1 | 4 |
| MCN stratification model | Benign/low risk | 19 | 0 | 0 |
| | Medium risk | 1 | 1 | 0 |
| | High risk | 1 | 0 | 4 |

Abbreviations: IPMN, intraductal papillary mucinous neoplasm; MCN, mucinous cystic neoplasm; NET, neuroendocrine tumor; SCN, serous cystadenoma; SPN, solid pseudopapillary; ESG, the European Study Group on Cystic Tumors of the Pancreas; ACG, the American College of Gastroenterology.

*ACG : For the ACG guideline, patients meeting any ACG-defined concerning criteria were classified as high risk, whereas those without these features were classified as low risk. The ACG guideline does not define a separate intermediate-risk category. For performance evaluation, pathologically confirmed low- and medium-risk lesions were combined into the non-high-risk group, whereas high-risk lesions were evaluated separately.

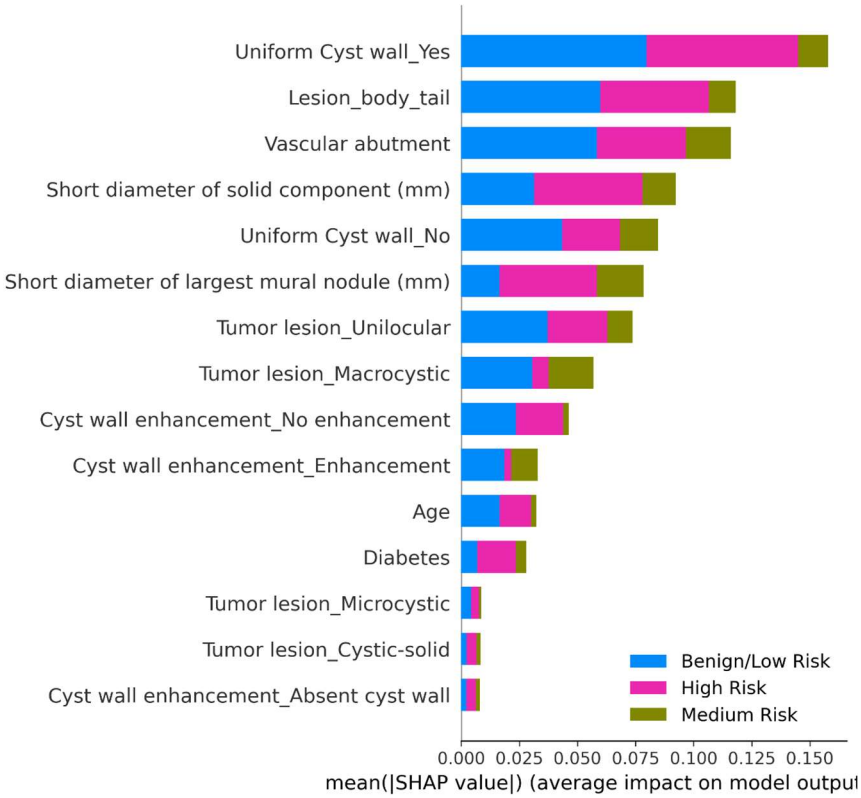

Figure S17. Feature importance analysis using SHAP values for the MCN risk stratification model. Mean absolute SHAP values showing the relative importance of clinical and imaging features in predicting MCN risk categories.

Stacked bar chart displaying the mean absolute SHAP (SHapley Additive exPlanations) values for each feature across three mucinous cystic neoplasm (MCN) risk categories: benign/low risk (blue), high risk (pink), and medium risk (olive). Features are ranked in descending order of overall importance. Uniform cyst wall (present) demonstrated the highest predictive value (mean |SHAP| ≈0.16), predominantly contributing to benign/low-risk classification. Lesion location in the pancreatic body-tail was the second most important feature, also favouring low-risk classification, consistent with the known predilection of MCN for this anatomical site. Vascular abutment and short diameter of solid component ranked third and fourth, contributing predominantly to high-risk classification. These findings align with established high-risk stigmata in current clinical guidelines. SHAP values were calculated directly from the final multinomial logistic regression model using a model-agnostic explanation approach to quantify the contribution of individual predictors to model predictions on the MCN cohort (Figure S16).

Forest plot presenting odds ratios (ORs) with 95 confidence intervals (CIs) for 16 clinical and imaging features across three MCN risk categories: low risk, medium risk, and high risk. For low-risk MCN, lesion location in the body-tail (OR 2.27, 95 CI 1.06–4.83), uniform cyst wall (OR 2.25, 95 CI 1.49–3.41), and unilocular morphology (OR 2.01, 95 CI 1.24–3.28) were significantly associated with benign/low-risk classification, whilst vascular abutment (OR 0.49, 95 CI 0.25–0.98) and non-uniform

cyst wall (OR 0.46, 95 CI 0.30–0.71) were inversely associated. For high-risk MCN, larger mural nodule diameter (OR 1.85, 95 CI 1.22–2.81) and larger solid component diameter (OR 1.66, 95 CI 1.23–2.24) were significantly associated with malignancy, whilst uniform cyst wall was protective (OR 0.50, 95 CI 0.30–0.82) (Figure S18).

Cross-tabulation of MCN risk stratification model is presented in Table S17, and related ROC curve is demonstrated in Figure S19.

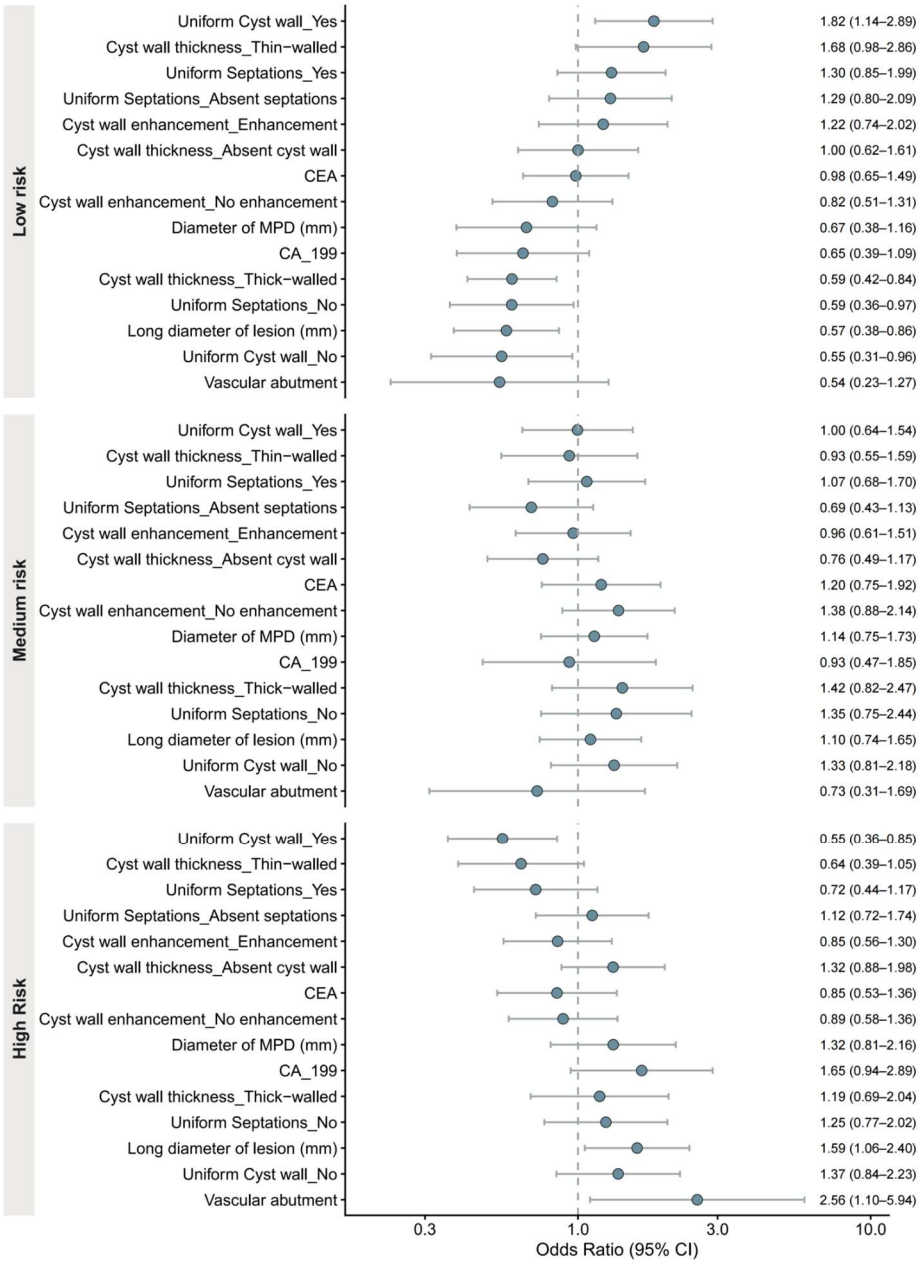

Figure S18. Forest plot of odds ratios for clinical and imaging features stratified by MCN risk category. Odds ratios and 95 confidence intervals for clinical and radiological features associated with low-risk, medium-risk, and high-risk mucinous cystic neoplasm (MCN) from multinomial logistic regression analysis.

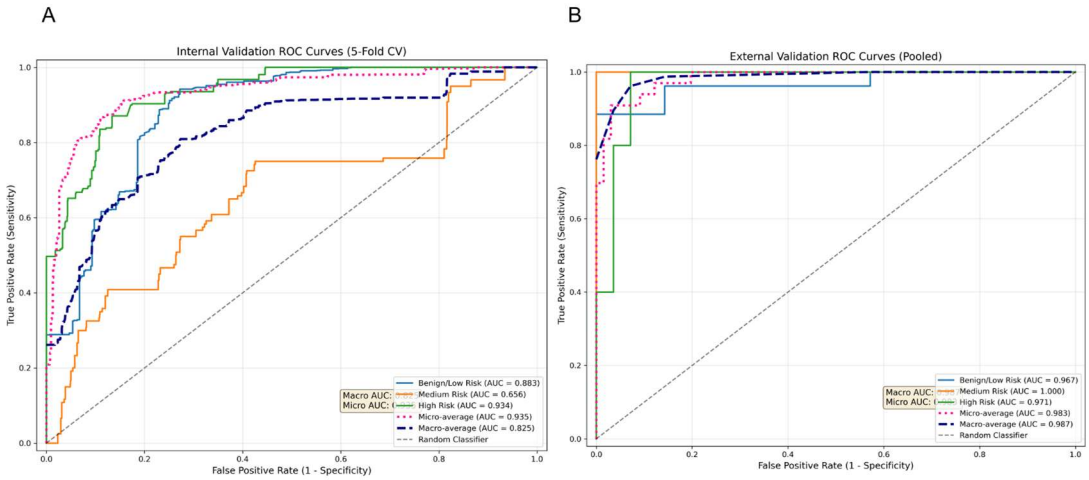


Figure S19. ROC curve of MCN for internal and temporal validation. (A) ROC curve of MCN for internal validation; (B) ROC curve of MCN for temporal validation.

We performed subgroup analyses according to imaging modality to assess the diagnostic performance of SIRS-PCL for MCN pathological risk prediction using CT- and MRI-based examinations. The corresponding results are presented in Table S18. Because only four patients underwent MRI in the temporal validation cohort, reliable confidence intervals could not be estimated owing to the limited sample size. Nevertheless, all four MRI cases were correctly classified as low-risk MCNs.

Table S18. Comparison of the diagnostic performance of CT- and MRI-based examinations for MCN pathological risk prediction in the complete cases of the temporal validation cohort

| Imaging | Class | Sensitivity | Specificity | AUC |
|---|---|---|---|---|
| CT | Benign/Low Risk | 0.88 (0.72-1.00) | 1.00 (1.00-1.00) | 0.98 (0.90-1.00) |
| | Medium Risk | 1.00 (1.00-1.00) | 0.95 (0.85-1.00) | 1.00 (1.00-1.00) |
| | High Risk | 1.00 (1.00-1.00) | 0.95 (0.84-1.00) | 0.99 (0.93-1.00) |
| MRI | Benign/Low Risk | — | — | — |
| | Medium Risk | — | — | — |
| | High Risk | — | — | — |

Abbreviation: CT, computed tomography; MRI, magnetic resonance imaging.

Note: Only four MRI cases were available in the temporal validation cohort; therefore, confidence intervals could not be reliably estimated because of the limited sample size.

**Appendix 7. Subgroup analysis conducted in full datasets without MICE**

Sensitivity analyses using complete-case datasets without MICE imputation demonstrated consistent performance across all three models. These findings suggest that MICE imputation did not introduce systematic bias and that the predictive performance of the SIRS-PCL is robust to missing data handling strategies.

For the five-category classification model, the overall AUC was comparable between the complete-case and MICE models (0.92 [0.89–0.94] vs. 0.93 [0.91–0.95]), with similar specificity (0.93 vs. 0.93), though the complete-case model showed lower overall sensitivity (0.51 vs. 0.66), largely attributable to reduced sensitivity for NET (0.30 vs. 0.50) and SPN (0.62 vs. 0.73) (Table S19).

Table S19. Comparison of complete-case and multiple-imputation analyses for five-class stratification model

| Cohort | Pathological risk stratification | Prediction performance | | |
|---|---|---|---|---|
| | | AUC (95 CI%) | Sensitivity | Specificity |
| Complete-case analysis | IPMN | 0.96 (0.93-0.98) | 0.72 | 0.94 |
| | MCN | 0.90 (0.86-0.94) | 0.43 | 0.87 |
| | SCN | 0.90 (0.86-0.94) | 0.50 | 0.91 |
| | SPN | 0.97 (0.94-0.99) | 0.62 | 0.98 |
| | NET | 0.85 (0.75-0.94) | 0.30 | 0.93 |
| | Overall | 0.92 (0.89-0.94) | 0.51 | 0.93 |
| MICE analysis | IPMN | 0.96 (0.93-0.98) | 0.90 | 0.90 |
| | MCN | 0.91 (0.87-0.95) | 0.54 | 0.90 |
| | SCN | 0.90 (0.87-0.94) | 0.62 | 0.91 |
| | NET | 0.87 (0.78-0.95) | 0.50 | 0.94 |
| | SPN | 0.98 (0.95-0.99) | 0.73 | 0.98 |
| | Overall | 0.93 (0.91-0.95) | 0.66 | 0.93 |

Abbreviations: AUC, area under the receiver operating characteristic curve; CI, confidence interval.

For the IPMN risk stratification model, performance was nearly identical between the two approaches, with mean AUC of 0.82 (0.73–0.91) for the complete-case model and 0.86 (0.79–0.93) for the MICE model, and comparable sensitivity and specificity for both low-risk and high-risk categories (Table S20).

Table S20. Comparison of complete-case and multiple-imputation analyses for the IPMN risk stratification model.

| Cohort | Pathological risk stratification | Prediction performance | | |
|---|---|---|---|---|
| | | AUC (95 CI%) | Sensitivity | Specificity |
| Complete-case analysis | Low risk | 0.83 (0.71-0.93) | 0.79 | 0.85 |
| | Medium risk | 0.73 (0.55-0.88) | 0.26 | 0.92 |
| | High risk | 0.91 (0.83-0.97) | 0.84 | 0.84 |
| | Mean | 0.82 (0.73-0.91) | 0.630 | 0.87 |
| MICE analysis | Low risk | 0.83 (0.73 to 0.92) | 0.73 | 0.81 |
| | Medium risk | 0.71 (0.56 to 0.86) | 0.33 | 0.91 |
| | High risk | 0.92 (0.85 to 0.97) | 0.87 | 0.90 |
| | Mean | 0.86 (0.79 to 0.93) | 0.65 | 0.87 |

Abbreviations: AUC, area under the receiver operating characteristic curve; CI, confidence interval.

For the MCN risk stratification model, both models achieved similarly high performance, with mean AUC of 0.98 (0.93–1.00) for the complete-case model and 0.97 (0.91–1.00) for the MICE model, and high sensitivity and specificity across all risk categories. These findings suggest that MICE imputation did not introduce systematic bias and that the predictive performance of the SIRS-PCL is robust to missing data handling strategies(Table S21).

Table S21. Comparison of complete-case and multiple-imputation analyses for the MCN risk stratification model.

| Cohort | Pathological risk stratification | Prediction performance | | |
|---|---|---|---|---|
| | | AUC (95 CI%) | Sensitivity | Specificity |
| Complete-case analysis | Benign/Low risk | 0.98 (0.93 to 1.00) | 0.91 | 1.00 |
| | Medium risk | 0.92 (0.80 to 1.00) | 1.00 | 0.92 |
| | High risk | 0.96 (0.86 to 1.00) | 0.75 | 0.96 |
| | Mean | 0.98 (0.93 to 1.00) | 0.89 | 0.96 |
| MICE analysis | Benign/Low risk | 0.97 (0.90 to 1.00) | 0.88 | 1.00 |
| | Medium risk | 1.00 (1.00 to 1.00) | 1.00 | 0.97 |
| | High risk | 0.97 (0.91 to 1.00) | 1.00 | 0.93 |
| | Mean | 0.97 (0.91 to 1.00) | 0.96 | 0.97 |

Abbreviations: AUC, area under the receiver operating characteristic curve; CI, confidence interval.

**Appendix 8. Clinical application of SIRS-PCLs: prospective data management and case demonstrations of pathological five-category classification and risk stratification**

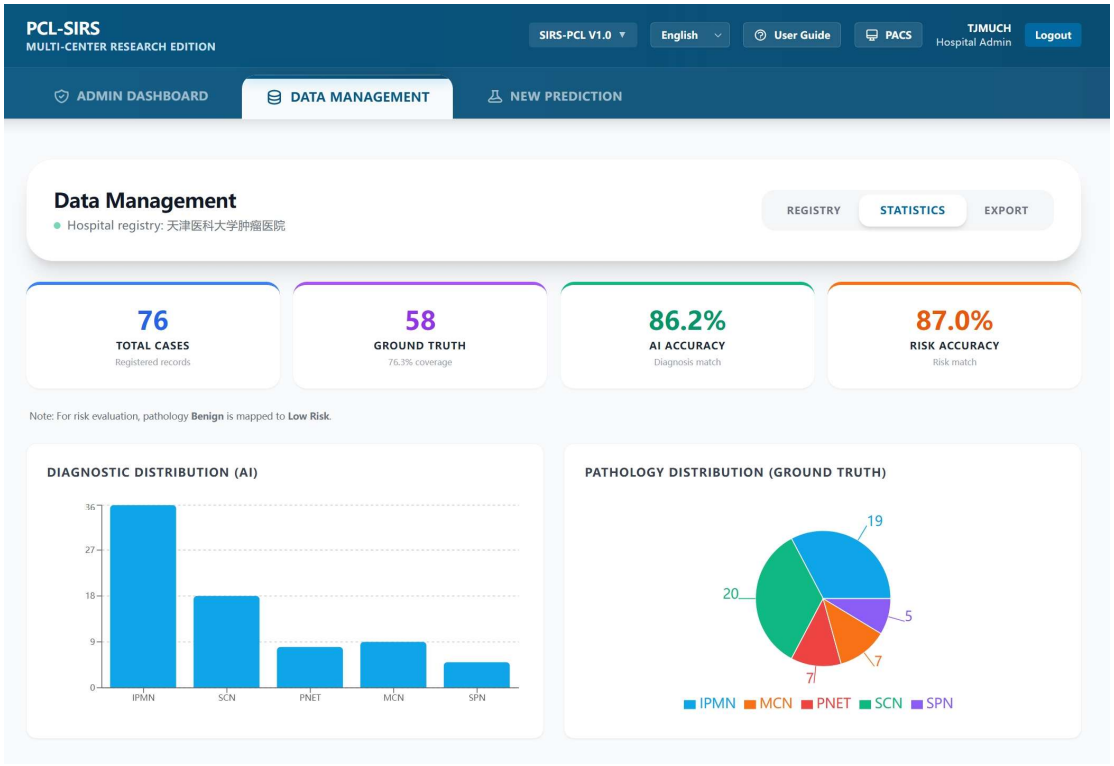


Figure S20. Prospective evaluation cohort in the SIRS-PCLs platform.

Dashboard view of the prospective cohort from Tianjin Medical University Cancer Institute and Hospital, including 76 registered patients with pancreatic cystic lesions, of whom 58 had pathologic reference diagnoses. The interface displays cohort-level diagnostic and risk-stratification accuracy, AI-predicted diagnostic distribution, and pathologic diagnostic distribution among cases with available ground truth. For risk evaluation, pathologic benign lesions were mapped to the low-risk category.

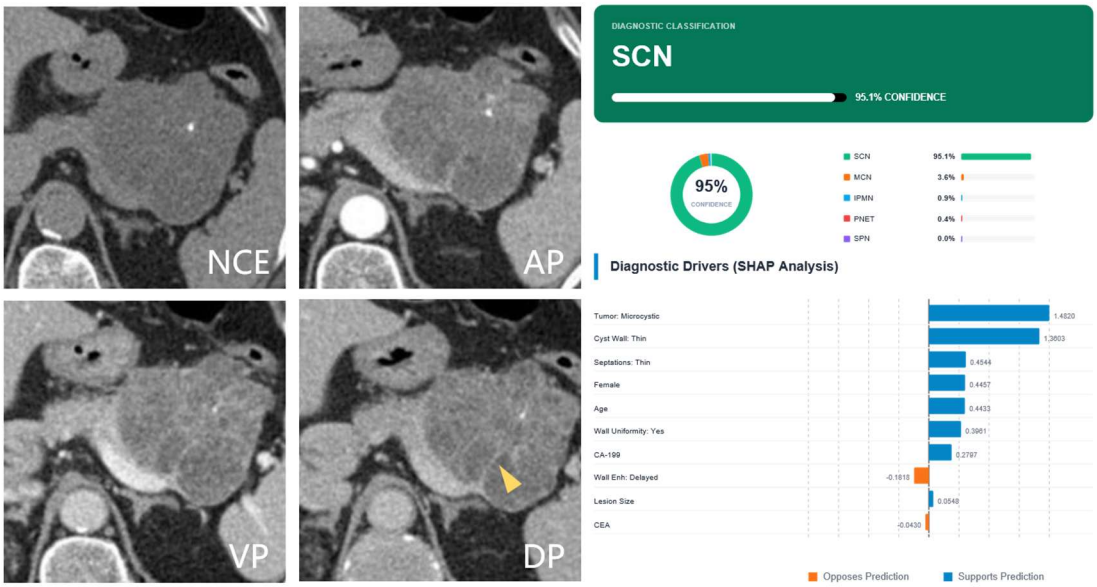


Figure S21. A 73-year-old female has a microcystic lesion (76 × 66 mm) located in the pancreatic tail, showing a thin uniform wall, thin uniform septation with delayed enhancement. The lesion does not communicate with the MPD and lacks a visible capsule. The CA19-9 is 0.60 U/mL, and CEA is 5.01 ng/mL.

**Model prediction:** SCN

**Histopathology:** (Pancreatic body and tail) Serous cystadenoma, microcystic type. Pancreatic resection margin (-)

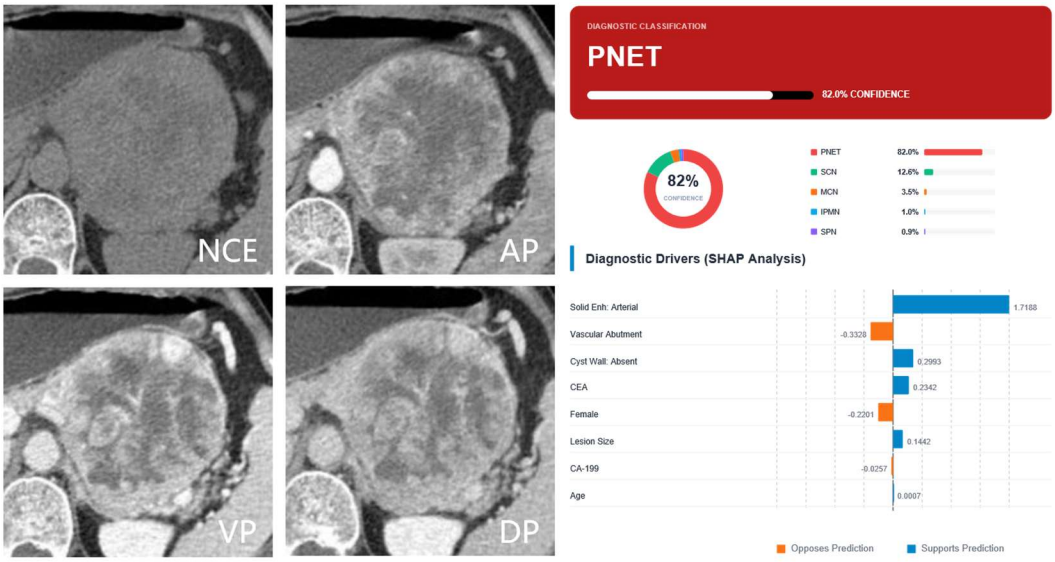


Figure S22. A 53-year-old female has a cystic-solid lesion (98 × 87 mm) located in the pancreatic tail, showing solid components with early enhancement during the arterial phase, and abutment of adjacent vessels. The lesion does not communicate with the MPD and lacks a visible wall. The CA19-9 is 22.25 U/mL, and CEA is 5.41 ng/mL.

**Model prediction:** PNET

**Histopathology:** (Pancreatic tail) Neuroendocrine tumor (NET), G1. Tumor tissue invasion into vascular walls observed. No regional lymph node metastasis identified; lymph node groups as follows: Station 8: 0/1, Station 9: 0/2, Splenic hilum: 0/1.

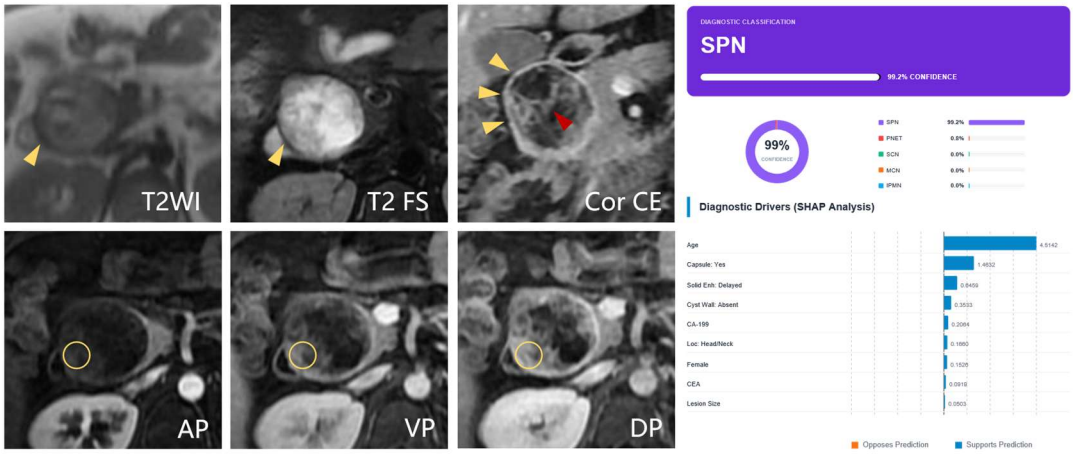


Figure S23: An 18-year-old female has a cystic-solid lesion (61 × 57 mm) located in the pancreatic head, showing a visible capsule, and solid components with delayed enhancement. The CA19-9 is 8.92 U/mL, and CEA is 1.52 ng/mL.

**Model prediction:** SPN

**Histopathology:** Solid pseudopapillary neoplasm of the pancreas with capsular invasion observed. Gastric resection margin (-), Pancreatic resection margin (-), Duodenal resection margin (-), Common bile duct resection margin (-), Major duodenal papilla (-), Lesser omental sac (-). No regional lymph node metastasis identified; lymph node groups as follows: Mesocolon 0/2, Station 8: 0/1, Greater curvature of stomach 0/1, Lesser curvature soft tissue (-).

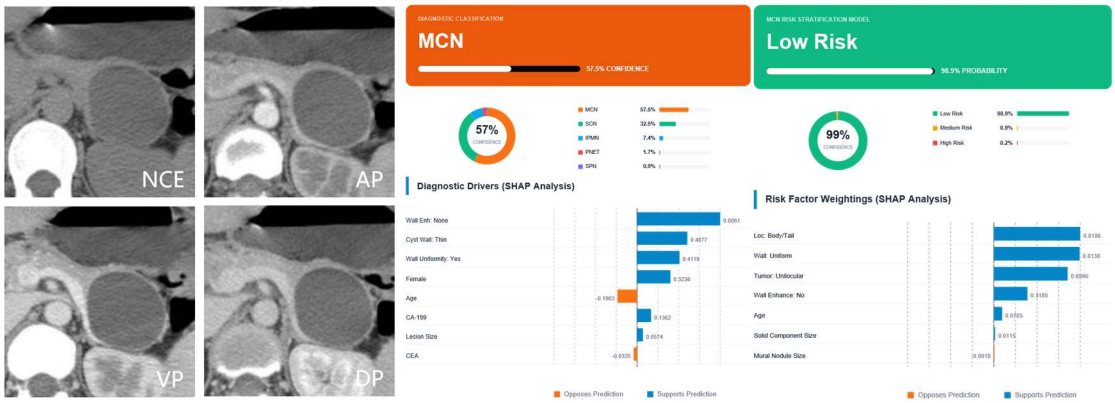


Figure S24. A 45-year-old female has a unilocular cystic lesion (54 × 49 mm) located in the pancreatic tail, showing a thin uniform wall without wall enhancement, septations, or mural nodules. The CA19-9 is 32.51 U/mL, and CEA is 0.97 ng/mL.

**Model prediction:** MCN, low risk

**Histopathology:** Mucinous cystic neoplasm with focal cyst wall fibrosis and calcification. Immunohistochemistry: Cytokeratin 19 (+), Cytokeratin 7 (+), Ki-67 (2%+), P53 (scattered +), CD31 (-), CD34 (-), Progesterone receptor (stromal +). Special stain: Periodic acid-Schiff (+)

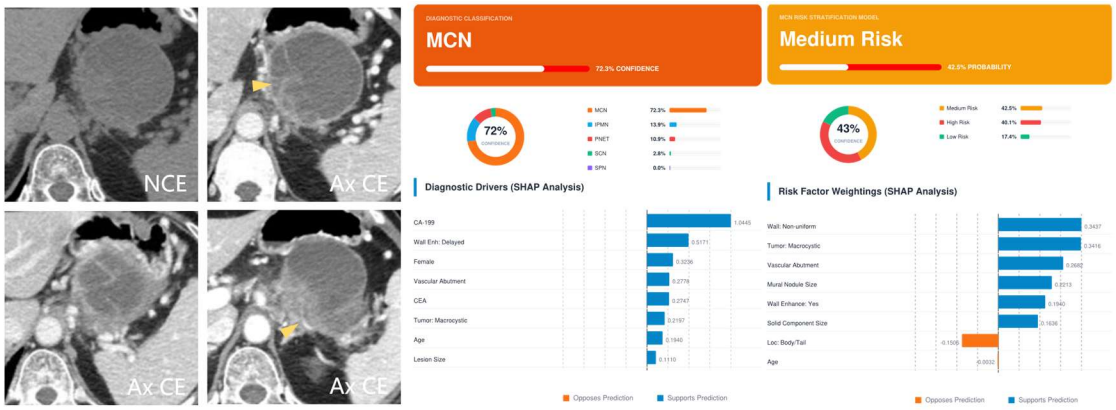


Figure S25. A 62-year-old female has a macrocystic lesion (63 × 63 mm) located in the pancreatic body and tail, showing a thick non-uniform wall with delayed enhancement, and abutment of adjacent vessels. The CA19-9 is 1494 U/mL, and CEA is 152.5 ng/mL.

**Model prediction:** MCN, medium risk

**Histopathology:** Multilocular mucinous cystadenoma with focal carcinoma in situ; clinical follow-up recommended. Pancreatic resection margin (-), Greater omentum (-), 3 peripancreatic lymph nodes demonstrating reactive hyperplasia. Immunohistochemistry: Ki-67 (2%+), Carcinoembryonic antigen (scattered +), P53 (individual cells +)

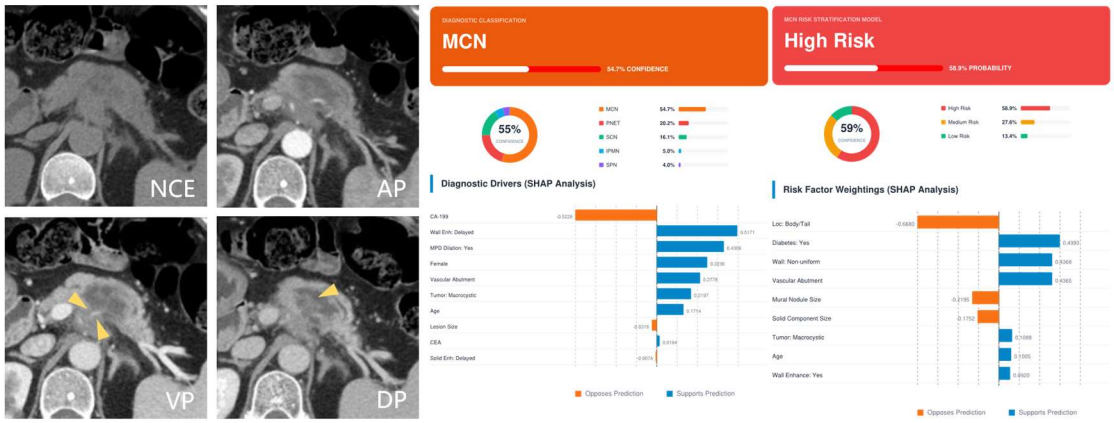


Figure S26. A 61-year-old female with diabetes has a macrocystic lesion (39 × 35 mm) located in the pancreatic body and tail, showing a thick non-uniform wall, thick non-uniform septations with delayed enhancement, MPD dilatation, and abutment of adjacent vessels. The CA19-9 is 1.13 U/mL, and CEA is 3.10 ng/mL.

**Model prediction:** MCN, high risk

**Histopathology:** (Pancreatic body and tail) Mucinous papillary cystadenoma with focal malignant transformation to mucinous adenocarcinoma, extending beyond the pancreatic capsule and involving surrounding adipose tissue. Pancreatic resection margin (-), Greater omentum (-), Hepatic portal soft tissue (-), Lesser omentum (-), Perirenal adipose capsule (-), Left adrenal gland (-). No regional lymph node metastasis identified; Immunohistochemistry: Cytokeratin 7 (+), Cytokeratin 19 (+), Chromogranin A (-), Synaptophysin (-), Ki-67 (focal 20%+), p63 (-), Vimentin (-). MLH1 (+), PMS2 (+), MSH2 (+), MSH6 (+).

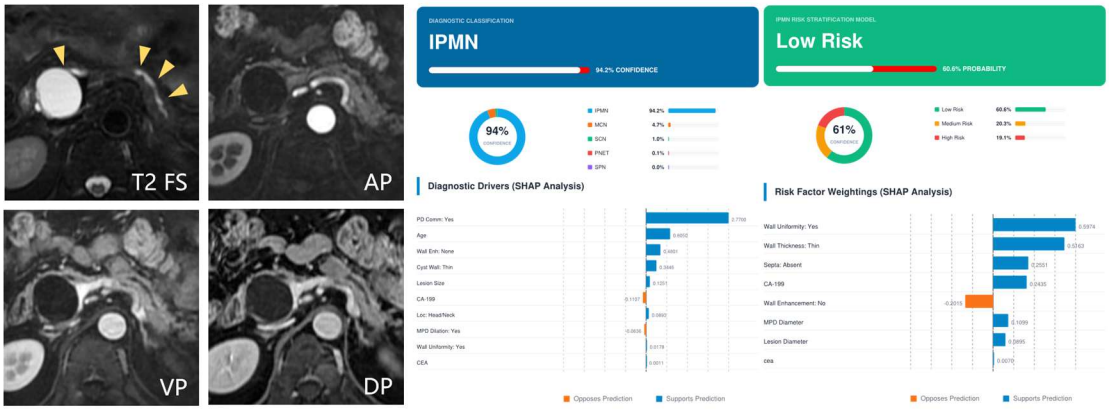


Figure S27. A 63-year-old male has a unilocular cystic lesion (35 × 33 mm) located in the pancreatic head, showing a thin uniform wall, communication with the MPD, and MPD dilatation, without wall enhancement or septations. The CA19-9 is 12.40 U/mL, and CEA is 2.21 ng/mL.

**Model prediction:** IPMN, low risk

**Histopathology:** Consistent with intraductal papillary mucinous neoplasm with mild atypical hyperplasia of glandular epithelium. Gastric, duodenal, common bile duct, and pancreatic resection margins all (-). Greater curvature of stomach, lesser curvature of stomach, suprapyloric, subpyloric, and peripancreatic soft tissues all (-). Immunohistochemistry: Cytokeratin 7 (+), Cytokeratin 19 (+), Alpha-1-antitrypsin (weak +), Alpha-1-antichymotrypsin (-), Chromogranin A (-), Synaptophysin (-), Ki-67 (1-2%+), CD10 (-), Progesterone receptor (-), Beta-catenin (membranous +), Vimentin (-)

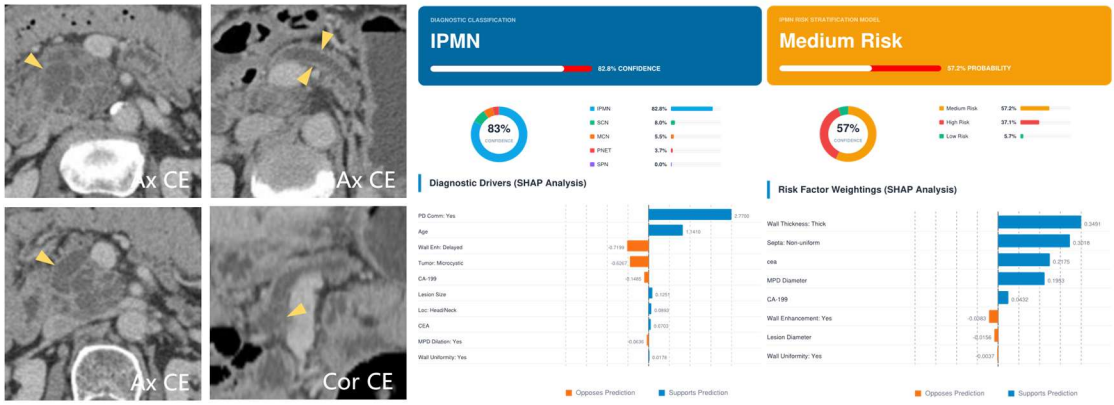


Figure S28. A 67-year-old male with diabetes has a microcystic lesion (56 × 41 mm) located in the pancreatic head, showing a thick uniform wall with delayed enhancement, thick non-uniform internal septations, communication with MPD, and MPD dilatation. The CA19-9 is 10.90 U/mL, and CEA is 7.65 ng/mL.

**Model prediction**: IPMN, medium risk

**Histopathology:** (Pancreatic head) Intraductal papillary mucinous neoplasm with intermediate-to-high grade dysplasia. Partially complex papillary branching with active cellular proliferation observed; close clinical follow-up recommended. Additionally, reactive hyperplasia identified in: 2 Station 3 lymph nodes, 2 Station 4 lymph nodes, 1 Station 5 lymph node, 1 Station 6 lymph node, 1 Station 8 lymph node, and 1 Station 13 lymph node. Immunohistochemistry: Cytokeratin 7 (+), Cytokeratin 19 (+), Alpha-1-antitrypsin (-), Alpha-1-antichymotrypsin (-), Chromogranin A (-), Synaptophysin (-), Ki-67 (5%+), Progesterone receptor (-), Beta-catenin (-), P53 (-).Special stain: Periodic acid-Schiff (+)

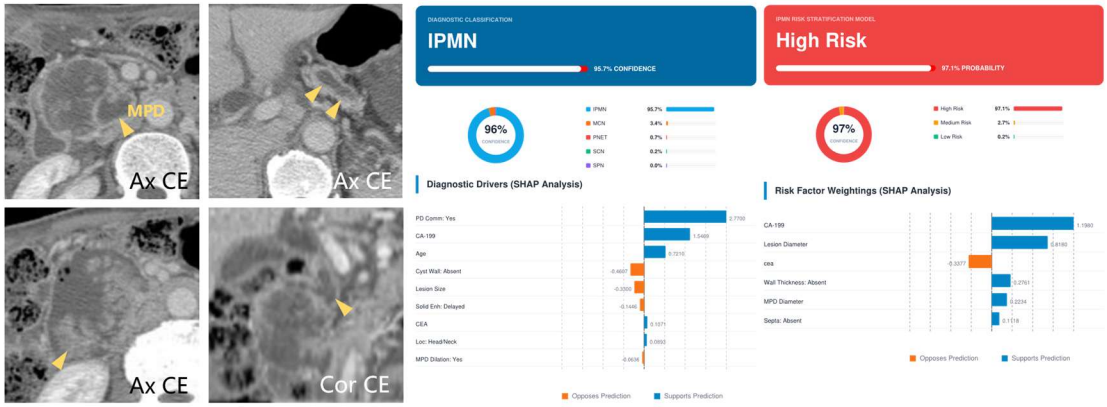


Figure S29. A 62-year-old male with jaundice and diabetes has a cystic-solid lesion (69 × 55 mm) located in the pancreatic head, showing solid components with delayed enhancement, communication with the MPD, and MPD dilatation. The CA19-9 is 2425 U/mL, and CEA is 13.66 ng/mL.

**Model prediction**: IPMN, high risk

**Histopathology:** (Pancreatic head) Intraductal papillary mucinous neoplasm with associated invasive carcinoma; the invasive component comprises moderately differentiated adenocarcinoma and mucinous adenocarcinoma, extending to invade the duodenal mucosal surface. Gastric resection margin (-), Duodenal resection margin (-), Pancreatic resection margin (-), Common bile duct resection margin (-). No regional lymph node metastasis identified; Immunohistochemistry: CDX-2 (-), Cytokeratin 7 (+), Ki-67 (50%+), MLH1 (+), PMS2 (+), MSH2 (+), MSH6 (+), MUC-1 (+), MUC-2 (+), MUC-6 (-).